DEVELOPMENT OF A TEST FACILITY FOR EVALUATION OF CONCRETE PAVEMENT JOINTS

By

CHARNCHAI SIRIWAT

Bachelor of Engineering
Chulalongkorn University
Bangkok, Thailand
1968

Master of Science
Oklahoma State University
Stillwater, Oklahoma
1972

Submitted to the Faculty of the Graduate College
of the Oklahoma State University
in partial fulfillment of the requirements
for the Degree of
DOCTOR OF PHILOSOPHY
December, 1987

DEVELOPMENT OF A TEST FACILITY FOR EVALUATION

OF CONCRETE PAVEMENT JOINTS

Thesis Approved:

John B. Lloyd
Thesis Advisor

W M Dawson

Roy C. Donley

Paul Zuerneman

R L Lowery

Norman N. Durham
Dean of the Graduate College

ACKNOWLEDGEMENTS

I wish to express my sincere gratitude to all the people who assisted me through all the stages and steps of my degree program at Oklahoma State University. In particular, I would like to express my appreciation to my major advisor, Dr. John P. Lloyd, for his calm assurance, patience, and ongoing support.

I am also thankful to Dr. Rex Donahey for his helpful suggestions on the development of data acquisition system software.

Special thanks are due to the following organizations for their supports: Institute of Technology and Vocational Education, Bangkok, Thailand; Office of the International Program, OSU; and Oklahoma Department of Transportation.

To Vachira Terayanont who walked the difficult steps with me through the whole process, I am grateful.

To my family and my wife, Panta, my deepest appreciation for their endless love and understanding.

TABLE OF CONTENTS

Chapter Page

LIST OF TABLES

LIST OF FIGURES

CHAPTER I

INTRODUCTION

1.1 Statement of the Problem

Transverse contraction joints are constructed in concrete pavements to relieve tensile stresses, and when properly spaced they control the location of transverse cracks. Proper spacing is determined principally by three factors: 1) the presence or absence of steel, 2) the environment, and 3) the properties of the aggregates.

Contraction joints are most frequently constructed by sawing or forming a narrow groove in the pavement to the depth required to produce a plane-of-weakness. For highway pavements, the minimum required depth of the groove is normally one-sixth of the slab thickness; sawed joints should meet the additional requirement that depth is not less than the diameter of the maximum size aggregate. At the plane-of-weakness, restrained contraction forces produce a crack below the groove (2).

In order to maintain an acceptable ride quality, the two pavement sections at a joint must remain at the same elevation while in service. This can be accomplished; 1) if the subgrade maintains the same elevation and stiffness on either side of the joint, or, 2) if the pavement joint itself can effectively transfer shear across the crack interface. This shear force is developed either by aggregate interlock, in which the aggregate particles at the faces of the joint transfer force, or by

a combination of aggregate interlock and load transfer through mechanical devices, such as dowel bars.

At the present time, most rigid pavements constructed in Oklahoma are unreinforced and undowelled and have sawed joints that are spaced at 15 feet. In private communication, engineers with the Oklahoma Department of Transportation have indicated that severe faulting of pavement joints, primarily in northeast Oklahoma, has been encountered after only a few years in service. Many factors can promote the occurrence of joint failure. However, when the coarse aggregate in the concrete has marginal freeze-thaw durability or resistance to abrasion, failure of the aggregate may contribute to the premature failure of joints.

Recent study at Oklahoma State University has indicated that high-strength concrete improves freeze-thaw durability of concrete made with marginal aggregate. In addition, a theory exists that high cement matrix strength improves shear transfer capability of concrete. However, with high-strength concrete, fracture is often through aggregate which may reduce the effectiveness of shear transfer at cracks and promote joint faulting in the case of pavements. No experimental work which considers the effect of high-strength concrete on joint behavior in concrete made with marginal aggregate has been found. The current investigation considers the effect of concrete quality on pavement joint behavior and durability.

1.2 Objectives and Scope

The overall objectives of the research funded by ODOT, are to establish the effectiveness of shear transfer mechanism by aggregate in-

terlock at contraction joints in highway pavement made with high-strength concretes and to determine the improvement in performance of pavement joints when the concrete is made with marginal aggregate and the strength of concrete is increased.

This study is part of the ODOT research project. Specific objectives for this study include:

1) development of a test system to load and monitor the test of pavement specimens and
2) development of a suggested test program to evaluate appropriate pavement parameters.

CHAPTER II

BACKGROUND

2.1 Introduction

A limited amount of research on shear transfer mechanism across cracks in plain concrete by aggregate interlock subjected to repeated loading has been done (8,13,17,23,24,29,31). Only a few investigations (8,23) considered low intensity applied loads such as encountered at contraction joints in highway pavement.

This chapter discusses previous experimental works, theories, and the summary of parameters affecting shear transfer mechanism. A review of high-strength concrete is also presented.

2.2 Experimental Research on Shear Transfer Mechanism

One of the first investigations which considered shear transfer across cracks in plain concrete was conducted by Fenwich and Paulay (12). They carried out monotonic static load tests on small, 3.5 by 3.5 in., precracked specimens as shown in Fig. 1. Crack widths, ranging from 0.002 to 0.015 in., were held constant for each specimen. Transverse loads were applied in increments. After every load increment, the crack width was adjusted using an external force which was normal to the crack plane. Because the specimens developed flexural cracks at low

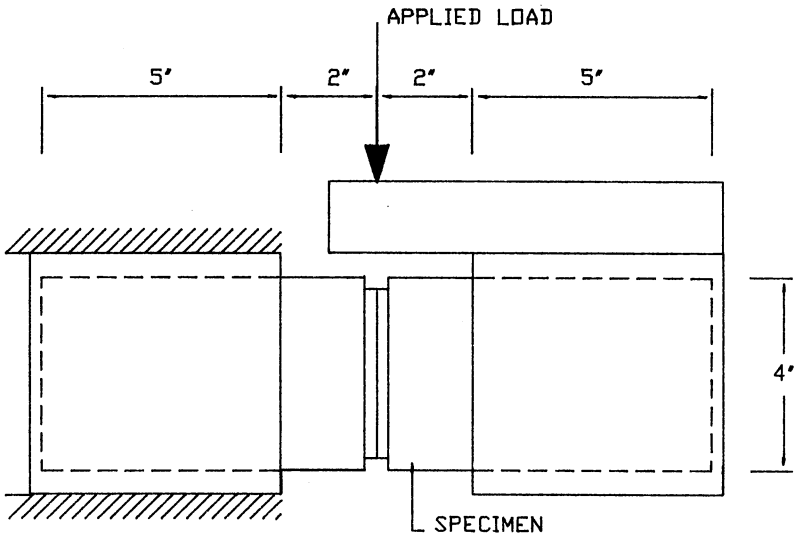

Figure 1. Test Setup Used by Fenwich and Paulay (12)

shear forces, the information obtained was of limited value.

In subsequent work, Paulay and Loeber (24) used a modified test setup and larger specimens designed to avoid early flexural tensile cracking. A total of 44 push-off type specimens were tested to evaluate the effects of crack width and aggregate shape and size on shear transfer. Specimens were tested using both monotonic and cyclic static loading. The specified crack widths were 0.005, 0.01, and 0.02 in. For cyclic load tests, extremely severe shear stresses of 830 psi were incrementally applied to each specimen 33 times. In the last cycle, the load was increased until failure occurred. Testing became impractical after the 17th cycle for the specimen with a 0.02 in. crack width. It was reported that, for all tests, there was no observed sudden break down of aggregate interlock. There was, however, an accumulation of residual shear displacements with progressive loading. These residual displacements increased proportionally with the crack width. It was observed that the shear stress-shear displacement relationship was essentially dependent on the crack width. Shape and size of the aggregate particles had no noticeable influence on the shear transfer mechanism.

Shear transfer across cracks in concrete was investigated experimentally by White and Holley (31). Sixteen 1.5 by 2.0 by 3.0 ft precracked concrete blocks were tested. In the test setup as shown in Fig. 2, each specimen was cracked to form two unconnected blocks which were separated to a preset crack width ranging from 0.015 to 0.030 in. Further separation of the two halves of the specimen was restricted by four external rods fastened to the blocks. Each block was subjected to reversing stresses applied by hydraulic rams in the range of $\pm$120 to $\pm$160

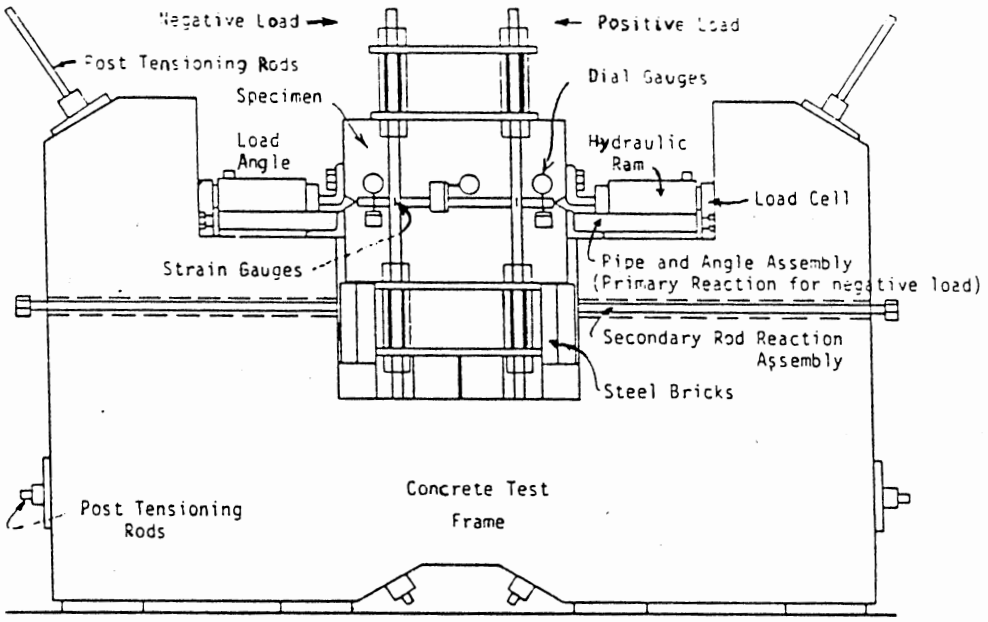

Figure 2. Test Setup Used by White and Holley (31) and by Laible, White, and Gergely (17)

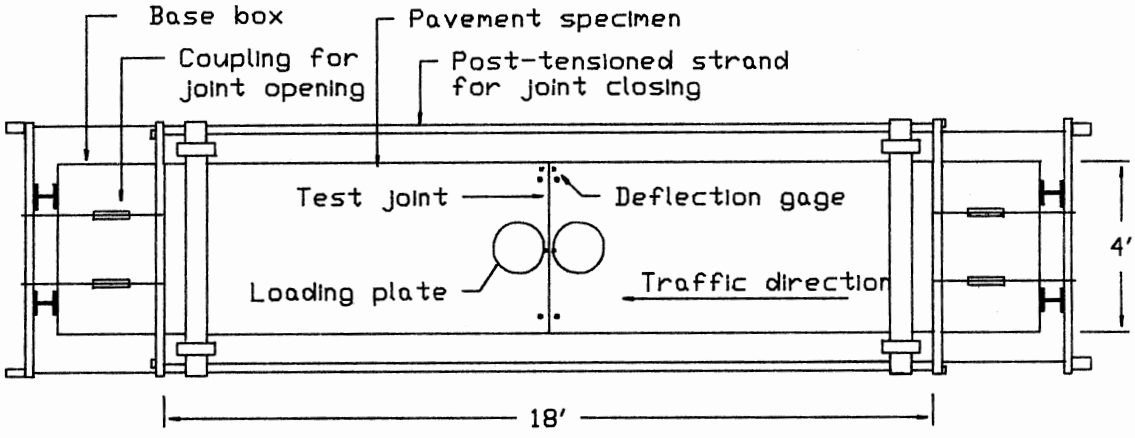

Figure 3. Test Setup Used by Colley and Humphrey (8) and by Nowlen (23)

psi for a maximum of 55 cycles. Specimens were then subjected to a monotonic load to failure. The primary response characteristics measured were slip along the crack, change in crack width during loading, and the magnitude of tensile clamping force in the external rods. Two concrete mixes were used, one with a coarse aggregate fraction in the size range of 1/2 in. to No. 4 (No. 7 aggregate according to ASTM C33) and the second with a coarse aggregate fraction ranging from 1 1/2 in. to No. 4 (ASTM size No. 467). A Los Angeles abrasion test (ASTM C131) conducted on the A grading portion of the coarse aggregate gave 21.8 percent wear at 500 revolutions. Both mixes used Type III high early strength portland cement. Nominal strength of the concrete was 3,000 psi. It was observed that no significant damage to the integrity of the shearing surfaces occurred during the cyclic loading of the specimens.

An extension of the work performed by White and Holley was conducted by Laible, White, and Gergely (17). Fully reversed cyclic shear stresses of about $\pm$180 psi were applied across preselected initial crack widths of 0.10, 0.20, and 0.30 in. for 25 cycles. Slip at the crack, increase in crack opening, and forces in the restraining rods normal to the crack were measured as functions of initial crack width, shear stress magnitude, cycles of shear stresses, restraining axial stiffness, concrete strength, aggregate properties, and age at loading. The preset crack widths and the external restraint stiffness appeared to have a significant influence on the displacements at the shear loading. In addition, the displacements were significantly larger if the concrete strength was lower or if the maximum aggregate size was decreased from 1.5 to 0.5 in.

Load transfer across joints in concrete pavements by aggregate interlock was investigated by Colley and Humphrey (8). Variables evaluated were the effect of the width of the joint opening, the thickness of the concrete slab, the magnitude of loading, the stiffness of foundation, and the shape of aggregate. In the test setup (Fig. 3), 7 to 9 in. thick slab specimens were cast on top of a supporting reinforced concrete box containing pavement foundation base. The 14-day compressive strength of the concrete averaged 5,500 psi. Load was applied at the joint using an electrically operated hydraulic system that alternatively pulsed the rams on either side of the joint. This was designed to simulate a train of truck wheels travelling across the joint. Each test consisted of 1,000,000 of these loads applied to a precracked specimen. Preselected joint opening widths, ranging from 0.025 to 0.085 in., were held constant during testing by adjusting crack width controlling devices (Fig. 3). Test results were summarized in terms of joint effectiveness and endurance index. The joint effectiveness E, was computed using the formula:

$$E\ (\%) = \frac{2d_i}{d_i + d_j}\ (100)$$

where d_i is the deflection of the unloaded slab and d_j is the deflection of the loaded slab. The endurance index of the joint performance was obtained by dividing the area under the curve of effectiveness vs cycles by the area that would be developed if the joint retained an effectiveness of 100 percent throughout one million load applications. The effectiveness of shear transfer was found to be drastically affected by the width of the crack and the stiffness of the foundation base.

Nowlen (23) extended the work to study the influence of aggregate size and hardness and age at time of joint cracking on load transfer effectiveness. The effect of aggregate size was studied with pavement section made with maximum aggregate sizes 3/4, 1 1/2, and 2 1/2 in. and joint width of 0.035 in. and 0.065 in. The effect of hardness was evaluated at 0.035 in. opening using three different aggregates with Los Angeles abrasion loss of 17, 28, and 46 percent. Test results indicated that large aggregates were beneficial in maintaining load transfer, especially for larger joint openings. Increasing aggregate hardness was also beneficial. In addition, age of concrete at the time of cracking was significant. It was concluded that for equal joint openings early fracture of the joint faces resulted in aggregate pullouts. This contributed to high initial joint effectiveness, and to good endurance of effectiveness under repeated loads.

In 1956, the Highway Research Boards administered a project called the AASHO Road Test to study the performance of pavement and bridge structures of known characteristics under moving loads of known magnitude and frequency (15). The Road Test was composed of separate major experiments: one relating to flexible pavement, one to rigid pavement with concrete surfacing, one to short-span bridges with steel beams, and one to short-span bridges with concrete beams. Ten lanes of the specially-constructed test facility were tested under controlled loading ranging from 2,000-lb single-axle loads in one lane to 48,000-lb tandem-axle loads in another. A total of 1,114,000 axle loads were applied to the surviving pavement. In the rigid pavement experiments, half of the rigid pavement sections were reinforced and were constructed with transverse contraction joints spaced at 40 ft, whereas the other half were

not reinforced and had 15-ft joint spacing. All of the transverse joints contained dowel bars for load transfer. During the two-year period of test traffic, no significant difference in performance was found between the otherwise equivalent 40-ft reinforced and 15-ft nonreinfoced sections. It was reported that faulting occasionally occurred at cracks but never at the doweled transverse joints.

A highly important by-product of the AASHO Road Test was the development of a new concept for the evaluation of pavement performance. The level of a particular pavement's ability to serve the travelling public was termed its serviceability. When a specified minimum degree of serviceability was reached, major maintenance or reconstruction was required. Other important findings resulting from the pavement performance study included information on the equivalencies of single and tandem axle arrangements. For example, the experiments showed that for a given loss in serviceability a rigid pavement would withstand about the same number of 29,000-lb tandem-axle loads as 18,000-lb single-axle loads.

Based on empirical relationships derived from the AASHO Road Test, the AASHTO Interim Guide for Design of Pavement Structures (1) was developed. The guide presents design procedures for any system of highways.

2.3 Theoretical Models of Shear Transfer Mechanisms

Several models have been proposed to explain or predict aggregate interlock behavior. One model (17) distinguishes between interlock due to "local roughness" and to "global roughness" of the crack face (Fig.

4a). This model postulates that local roughness causes interlocking of the fine aggregate particles, principally a bearing or crushing action, while global roughness causes interlocking of the coarse aggregate particles, principally a sliding and overriding action. It is further postulated that the local roughness predominates in the early loading cycles, particularly in the first cycle and is the primary mode of shear transfer in all cycles when the initial crack width is less than 0.010 in. In contrast, global roughness predominates in later cycles and at wider initial crack widths. In this model, the surface roughness can be characterized by the variation of the slopes of the crack surface from a mean value of zero. Protuberances from the surface with high slope will have early contact with the surface on the other side of a crack when a shear load is applied (Fig. 4a). Experimental evidence (17) shows that there is a direct correlation between measured values of surface slope and the amount of slip.

An alternative model proposes that aggregate interlock is entirely due to frictional sliding of two rigid surfaces (Fig. 4b). These surfaces have been represented by a sawtooth shape (5) and by a series of parabolic segments (13).

A more recent model (29) suggests that concrete is a two-phase material of aggregate and cement matrix which can be modelled as a distribution of rigid spheres embedded within a deformable rigid-plastic matrix. Shear forces and direct compression forces for a given shear displacement and crack width increase are obtained from equilibrium. Hence, for a known direct stiffness restraining the width of a crack, the crack displacement path and shear stiffness can be obtained. A complex expression to predict the probability of a particular size of ag-

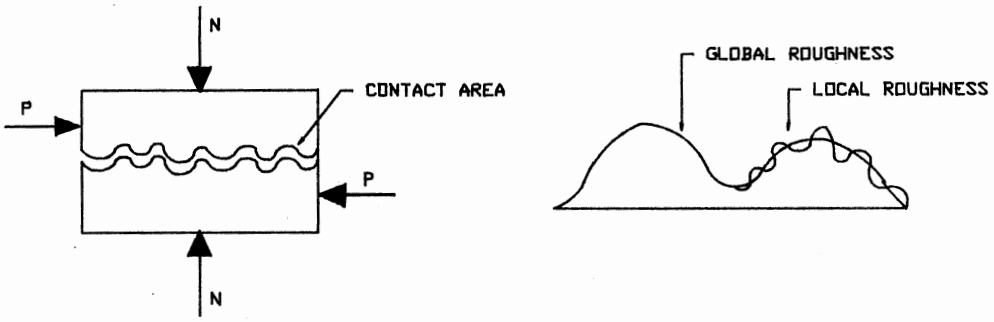

a) Local-Global Roughness Model (17)

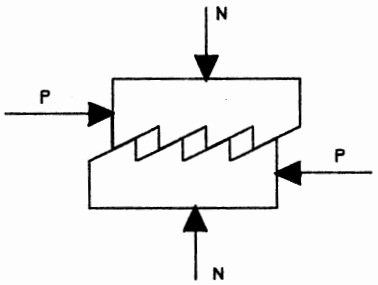

b) Shear-Friction Model (5)

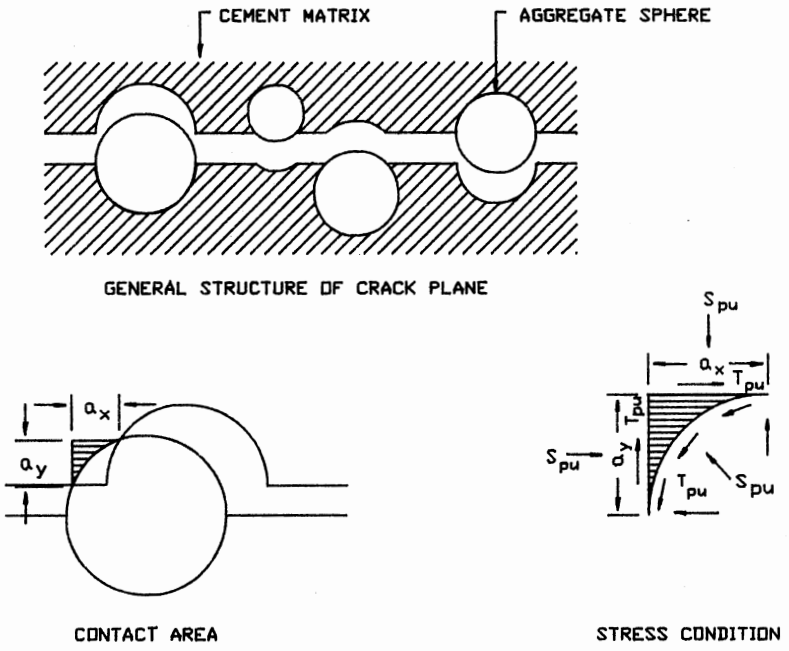

c) Two-Phase Material Model (29)

Figure 4. Models of Shear Transfer Mechanism

gregate particle at a particular embedment depth is derived. A simpler bilinear expression is also presented. In this model, the shear forces are resisted by a combination of crushing and sliding of the rigid spheres into and over a softer cement matrix (Fig. 4c). Contact and interaction between spheres projecting from opposite crack faces is not considered.

2.4 Summary of Factors Affecting Shear Transfer Strength

2.4.1 Introduction

From previous studies, it is known that there are a few dominant variables which influence the behavior of cracked concrete under shear and normal forces. These variables are, among others, the magnitude of the shear stress at the crack interface, the width of the joint, the restraining stiffness, the concrete strength, the roughness of the crack plane, and the hardness of the aggregates.

2.4.2 Effect of Shear Stress Magnitude

As shown in Fig. 5, for a given initial crack width and stiffness, the relationship between cyclic shear stress and peak slip can be represented approximately by a straight line (17,31). Laible, White, and Gergely (17) reported that shear resistance at high cycle numbers (15 or greater) at a stress level of $\pm$180 psi is somewhat insensitive to the previous loading history as long as the stresses remain in the range of 100-180 psi. Test results from Colley and Humphrey (8) show that there are significant differences in shear transfer behavior under the action

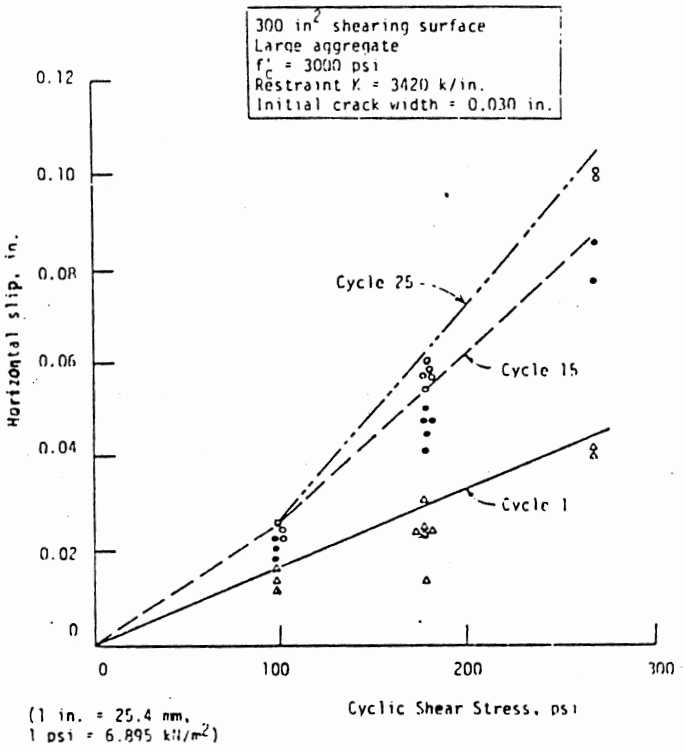

Figure 5. Effect of Shear Stress Magnitude (17)

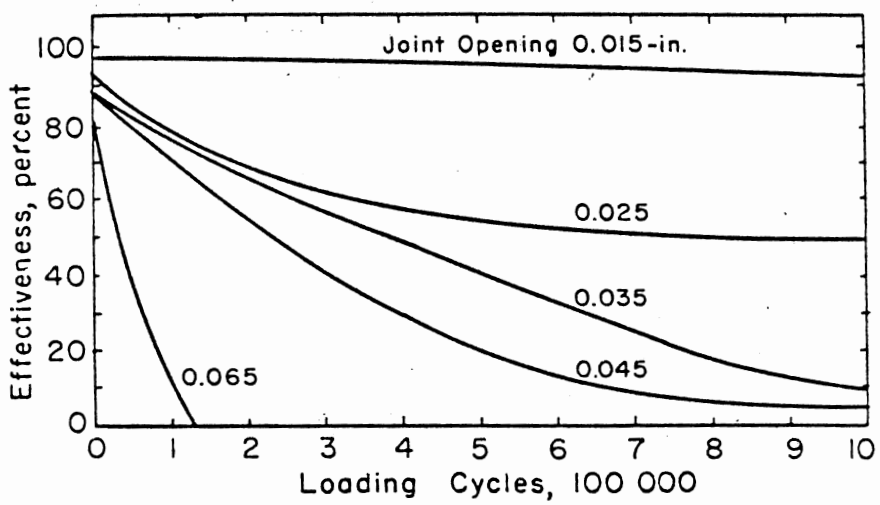

Figure 6. Effect of Crack Width (8)

of repetitive loading. After 500,000 loading cycles, the effectiveness of the joints tested at 0.035 in. joint opening with shear stresses of 27, 38, and 50 psi repetitive load was 96, 68, and 39 percent, respectively. After one million loading cycles, the effectiveness were 98, 65, and 9 percent. At the end of routine testing, one million additional load cycles were applied to the slab tested with the 27 psi load and there was no further change in effectiveness. This suggests that light loads cause little or no wear and probably do not need to be considered.

2.4.3 Effect of Crack width

When expansion joints are used only at structures or are widely spaced, the opening of a contraction joint depends primarily on spacing between joints and environment. Table I presents measurements of pavement joint openings over a 10-year period (8) showing the relationship between maximum opening, spacing, and geographical location.

Based on ten years of field data collection in Wisconsin, Shober (26) proposed a predictive expression for the average pavement joint opening in inches expected from the warmest to coldest temperature to be 0.0448 + 0.0044 * joint spacing in feet.

All available data (17,24,31) are in agreement that the peak slip values increase sharply with increasing initial crack widths because the surface deterioration is much more rapid for higher values of crack width. As shown in Fig. 6, the effectiveness of shear transfer for low intensity, approximately 30 to 40 psi loading of up to one million cycles was found to be drastically affected by the width of the joint opening (8). It appears that test specimens with low initial crack

widths of less than 0.010 in. behave much differently from the other specimens, in that both the initial ratio of slip to crack width and the rate of increase in slip/crack width ratio are much less severe than for the specimens with initial crack width of 0.020 in. or higher (17).

TABLE I

FIELD MEASUREMENTS OF JOINT OPENINGS

Location	Joint spacing (ft)	Maximum opening (in.)
Michigan	10	0.06
Michigan	20	0.08
California	15	0.03
Oregon	15	0.06
Kentucky	20	0.05
Missouri	25	0.07
Minnesota	15	0.07

The effect of joint opening and closing on the fit between worn aggregate particles in the fractured faces of the joint is also important to load transfer. As shown in Fig. 7, an increase in effectiveness is obtained when a joint is closed, then opened. It was pointed out by Colley (8) that this effect of aggregate fit and attrition explained in

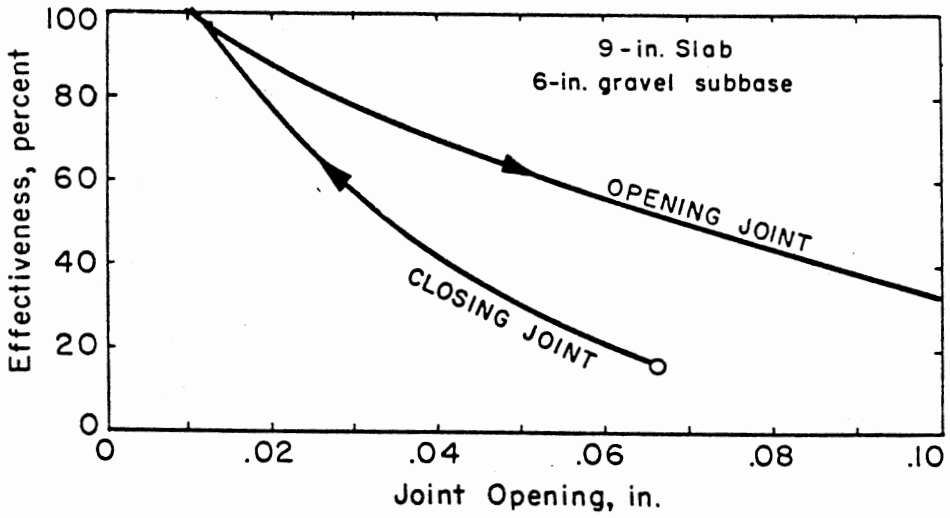

Figure 7. Effect of Joint Opening and Closing (8)

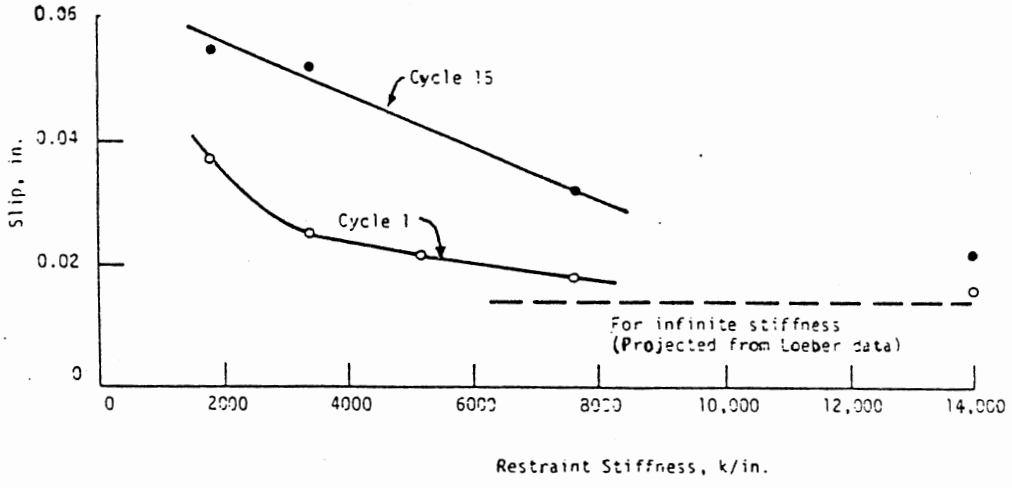

Figure 8. Relationship Between Shear Displacement and Restraint Stiffness (17)

part the good effectiveness values obtained for in-service highway joints that developed wide winter openings.

2.4.4 Effect of Restraint Stiffness

Although increased restraining stiffness decreases shear slip, it becomes less effective at high levels of restraint stiffness, above 10 ksi/in., for initial loading cycles. At the higher cycle numbers, an increase in restraint stiffness is more effective than during the initial cycle loadings (17).

Fig. 8 shows the relationship between shear displacement and restraint stiffness taken from Ref. 17. Shear displacement at infinite stiffness was projected from data of Ref. 8.

The restraint bar forces developed at a fixed shear stress decreased with decreasing initial crack width as shown in Table II, reported by Laible, White, and Gergely (17).

2.4.5 Effect of Aggregate Quality

2.4.5.1 Size and Gradation. Larger aggregate size has been reported to enhance the shear capacity, especially for larger joint openings (17,23). After one million cycles of loading, Nowlen (23) reported that an increase in nominal maximum aggregate size from 0.75 to 1.50 in. improved effectiveness by 11 percent for a 0.035 in. wide joint, while the increase gave no significant improvement in the effectiveness of a 0.065 in. wide joint. However, a further increase in aggregate size to 2.50 in. did improved the effectiveness for both the 0.035 and 0.065 in. joint openings. Although the shear stress is influenced by aggregate size and gradation, the normal stress is not very sensitive to the vari-

ation in size (29). Paulay and Loeber (24) found no noticeable effect of the aggregate size in the range of 3/8 to 3/4 in. used in their tests on the behavior of the shear transfer.

TABLE II

RELATIONSHIP BETWEEN INITIAL CRACK WIDTH AND RESTRAINING FORCE

Initial crack width in.	Ratio of total restraining force to applied shear force	
	Cycle 1	Cycle 15
0.030	30 - 40%	40 - 65%
0.020	30 - 40%	40 - 55%
0.010	10 - 20%	20 - 35%

2.4.5.2 Hardness and Abrasion. The use of hard aggregates is of significant value (17,20) for joint effectiveness. It can be postulated that interlock of aggregates deteriorates by abrasion. It would follow, then, that hard materials that are resistive to abrasion should maintain load transfer effectiveness longer than soft materials that abrade readily. Test results of three different aggregates with 17, 28 and 46 wearing percentage (ASTM C 131) confirmed that joints built with aggre-

gates with the lowest abrasion loss are superior in effectiveness endurance (23).

High quality aggregate maintains the shear capacity as the joint ages. A weak aggregate results in a decrease in shear resistance with age due to the increase in the amount of aggregate fracture. Stronger aggregate tends to pull out instead of fracturing, thereby producing a rougher surface and providing better load transfer (17).

2.4.6 Effect of Concrete Strength

Concrete strength and roughness of the crack are certainly not independent and determine the interlock resistance and crack opening during sliding. The resistance of the crack faces against shear displacements is most of all governed by the strength of the concrete (25,29). It was suggested that if the concrete strength is high, this is attended with a high matrix strength; as a result, the resistance against deformation of the contact areas is larger so that a higher shear stiffness is obtained. However, Millard and Johnson (21) reported that increase of the strength of concrete from 4.25 to 7.40 ksi had only a small effect upon the shear transfer. Also, caution was made that high strength concrete design alone does not affect the shear capacity. Poor quality control on an otherwise properly designed mix reduces the shear capacity, particularly in the first cycle when the lower strength cement paste leads to easier crushing (17).

2.5 High-Strength Concretes

2.5.1 Introduction

High-strength concretes represent a relatively new material which is now finding rapidly increasing use. The growth has been possible as a result of recent developments in material technology and a demand for higher-strength concrete. As the development has continued, the definition of high strength concrete has changed over the years. The definition adopted by the ACI Committee 363 (3) reads:

> The immediate concern of the Committee 363 shall be concretes have specified compressive strengths for design of 6000 psi (41 Mpa) or greater, but for the present time, considerations shall not include concrete made using exotic materials or techniques.

The current design practice is based, among other things, on experiments made with concrete of compressive strength in the range 3000-6000 psi. Additional considerations, modifications of the empirical equations, and new tests may be necessary before a satisfactory procedure for the design of structures made with concrete of compressive strength higher than 6000 psi is developed.

The measure of high strength concretes is generally the uniaxial compressive strength. For concrete with the normal compressive strength range, less than 6000 psi, it is generally assumed that the higher the strength, the higher the overall qualities of concretes. Many other properties of concrete such as tensile, shear, and bond strength are expressed in terms of the compressive strength. It was pointed out by Wittman (32) that one cannot always assume, especially for high-strength concrete, that high strength also means superior other properties, for example ductility. Thus it may be misleading to use uniaxial compres-

sive strength alone as the parameter when discussing high-strength concrete.

The economic advantages of using high-strength concrete for the column and shear walls of high-rise buildings have been demonstrated already in buildings such as the Water Tower Place in Chicago. In general, high-strength concrete can be and has been advantageously used for:

1) column and shear walls of high-rise buildings,
2) elevated structures,
3) precast and prestressed products, and
4) construction where durability (low porosity) is critical.

2.5.2 Selection of Materials

With the conventional methods of production and materials of construction, more stringent quality control, use of admixtures such as plasticizer and fly ash, and careful selection of the blends of cement and the type and size of aggregates are essential for high-strength concrete production.

2.5.2.1 Cement. The choice of a brand and type of portland cement is probably the most important factor in the selection of materials for high-strength concrete mixtures. Variations in compound composition and fineness that are permitted by ASTM C 150 will cause the concrete compressive strength to fluctuate more than any other single material, and these variations appear to have greater effect in high strength concrete (6). Unless high initial strength is required, there is no need to use a Type III cement. The development of high strength concrete

will require the utilization of a portland cement of optimum quality from a strength and workability standpoint. A program for studying variations in chemical and physical properties on locally available cements is a necessity.

A further consideration is the optimization of the cement-admixture system. The exact effect of a water-reducing agent on water requirement, for example, will depend on the cement characteristics. Strength development will depend on both cement characteristics and cement content.

2.5.2.2 Admixtures. Chemical admixtures, whether they are Type A, water reducing, Types F and G, high-range water reducer, or Type D, water reducing retarding, must conform to the requirements of ASTM C 494. Admixture compatibility with the preselected materials is important; therefore, job conditions should be closely simulated in the evaluation.

The use of air entrainment is recommended to enhance durability when concrete will be subjected to freezing and thawing while wet. As compressive strengths increase and water-cement ratios decrease, air-void parameters improve and entrained air percentages can be set at the lower limits of the acceptable ranges as given in ACI 201. Entrained air has the effect of reducing strength, particularly in high-strength mixtures, and for this reason it has been used only where there is a concern for durability (3).

Use of combinations of high-range water reducers with normal-setting water reducers or retarders have become common to achieve optimum performance at lower cost. Improvements in strength gain and con-

trol of setting times and workability are possible with optimized combinations.

The use of a good quality fly ash either Type F or Type C, meeting specifications of ASTM C 618, has been used in the production of high-strength concrete. Silica fume, which is by-products of silicon and ferrosilicon metals consisting of extremely fine particles about 0.15 microns in average size with a SiO_2 content from 85 to 98 percent, has also been used in high-strength concretes and has been applied not only for structural purposes but also for structure surfaces and repair materials in situation where high compressive strength and low permeability are advantages.

2.5.2.3 Aggregates. Careful consideration has been given to the shape, surface texture, and mineralogy of the coarse aggregate. It is well known that shape and surface texture affect the total mixing water requirements. These characteristics, along with the mineralogy of the aggregate, control the paste to aggregate bond and, therefore, play a great role in the strength producing qualities in high-strength concrete. Studies have indicated that for optimum compressive strength with high cement and low water to cement ratios the maximum size of aggregate should be kept to a minimum, at 1/2 in. or 3/8 in. Maximum sizes of 3/4 in. and 1 in. also have been used successfully.

One of the primary functions of fine aggregate in conventional concrete is its role in providing workability. Since high-strength concretes typically contain high contents of fine cementitious materials, the sands that provide good finishing characteristics in regular concrete are not as necessary. One report (6) stated that sand with a

fineness modulus around 2.5 produced concrete with sticky characteristics, which resulted in loss of workability and higher water demands. Sand with a fineness modulus of about 3.0 provided the best workability and compressive strength.

2.5.2.4 Water. The requirements for water quality for high-strength concrete are no more stringent than those for conventional concrete. Various sources of water that meet the limitations listed in ASTM C 94, have been used without detrimental effect on high-strength concrete mixtures.

2.5.3 Concrete Mix Proportions

Concrete mix proportions for high-strength concrete have varied widely. Influencing factors includes strength required, test age, characteristics of materials, and type of application. High-strength concrete mix proportioning is a more critical process than the design of normal concrete mixtures. Usually, specially selected pozzolanic and chemical admixtures are employed, and the attainment of a low water-cement ratio is considered essential. Many trial batches are often required to generate data that enable the researcher to identify optimum mix proportions.

2.5.3.1 Strength Required. The ACI Building Code Requirements for Reinforced Concrete (ACI 318) states that the concrete will be satisfactory when the average of all sets of three consecutive strength test results equals or exceeds the required strength and no individual strength test result falls below the required strength by more than 500 psi. To meet the requirements, the average strength must be higher than

the specified strength. The level of design strength is governed by the control of the variables that effect the compressive strength. A high variance in test results will dictate a higher required average strength. In most cases, a coefficient of variation of less than 10 percent would be necessary when producing high-strength concrete. Values higher than this would not only result in a very uneconomical mixture, but may very well require a design level which cannot be met.

2.5.3.2 Test Age. The selection of mix proportions can be influenced by the testing age, the age at which the acceptance criteria are established. Generally, concretes which develop high later-age strengths will also produce high early-age strengths. However, the optimum mix proportions may vary for different test ages. For example, Type III cement and no fly ash have been employed in a high early-strength design, compared to Type I cement and fly ash for a later-age strength design. High-strength concrete tests show that a considerable strength gain after 28 days is achieved. In order to take advantage of this fact, high-strength concretes are frequently tested at later ages such as 56 or 90 days.

2.5.3.3 Water-cement Ratio. Many researchers indicate that water-cement ratio is the single most important factor affecting the producibility of high-strength concrete. The same relationship between water-cement ratio and compressive strength in normal-strength concrete also exists in high-strength concrete. When pozzolanic materials are used in concrete, a water-cement plus pozzolan ratio by weight has been used in place of the traditional water-cement ratio by weight.

The slump of the concrete is related to the water-cement ratio and

the total amount of water in the concrete. Special consolidation efforts are usually required for 0 to 2 in. slump concrete. Lower water-cementitious ratios and higher slumps have been reported with the use of high-range water reducers. The production of high-strength concrete typically requires a water-cementitious ratio in the range from 0.27 to 0.50 (3).

2.5.3.4 Cement Content. The optimum cement content is best obtained through a series of trial batches. Common cement contents in high-strength concrete test programs range from 660 to 940 lb per cu.yd.

The strength efficiency per pound of cement is influenced by all of the variables which affect the strength of concrete. Higher cement efficiencies are achieved at high strength levels with lower maximum aggregate sizes (6).

2.5.3.5 Aggregate Proportions. In the proportioning of high-strength concrete, the aggregates have been a very important consideration since they occupy the largest volume of any of the ingredients in the concrete. It is generally agreed that the fine aggregates or sand have considerably more impact on mix proportions than the coarse aggregates. The fine aggregates contain much higher surface area for a given weight than do the larger coarse aggregates. Since the surface area of all aggregates must be coated with a cementitious paste, the proportion of fine to coarse can have a direct quantitative effect on paste requirements. Normally more economical and higher strength mixtures are obtained for a given amount of cementitious materials when using low fine aggregate contents with high coarse aggregate contents. However, if the proportion of sand is too low, serious problems in workability

become apparent (3).

2.5.3.6 Admixtures. Variations in dosage rates from the standard recommendations of the admixture manufacturer should be examined. Increased dosage as high as 50 percent above the amount recommended by the admixture manufacturer has resulted in substantial increases in compressive strength without detriment effects (6), however, caution should be taken when using lignosulfonates at an overdose, as they tend to entrain air in excess of 3 percent, which could reduce compressive strength substantially.

2.5.4 Properties

2.5.4.1 Stress-Strain Behavior. Properties of concrete such as stress-strain relationship, modulus of elasticity, tensile strength, shear strength, and bond strength are often expressed empirically in terms of uniaxial compressive strength. Typical axial stress-strain curves for concrete of compressive stress up to 12,000 psi are shown in Fig. 9. As the strength of the concrete is higher, the shape of the ascending part of the curve becomes more linear and steeper, and the strain at the maximum stress is slightly higher. In addition, high strength concrete exhibits less internal micro-cracking than normal strength concrete for a given imposed axial strain. Consequently, the relative increase in lateral strain is less for high-strength concrete (7).

2.5.4.2 Freeze-Thaw Resistance. Contradictory information about air content requirement for high-strength concrete to produce adequate durability is reported by the ACI Committee 363. They cited the conclu-

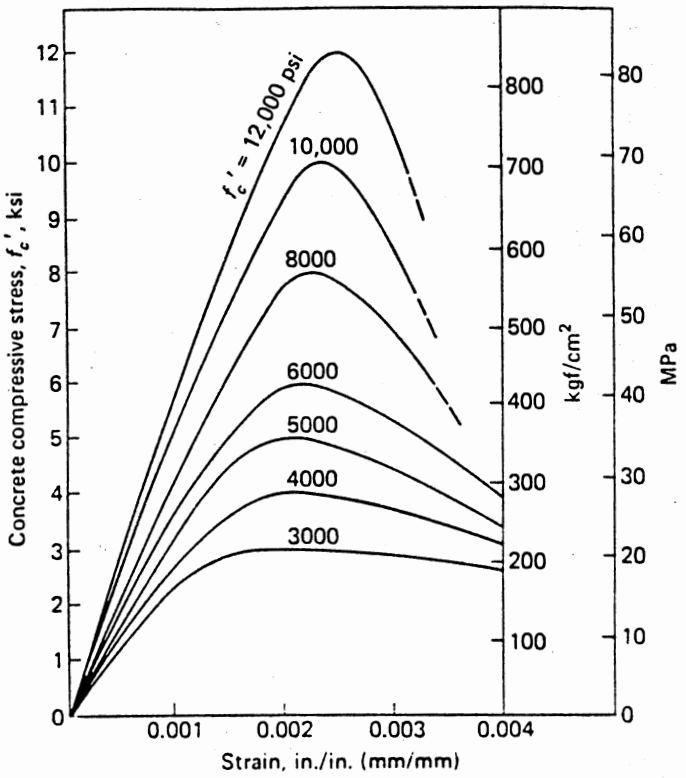

Figure 9. Stress-Strain Curves of High-Strength Concrete (30)

sion made by Saucier, Tynes, and Smith from their accelerated laboratory test that air-entraining should be considered for high-strength concrete under freezing and thawing conditions, in contrast to excellent freeze-thaw resistance of non-air entrained high-strength concrete obtained by Perenchio and Klieger (3).

2.5.5 Applications

Most applications of high-strength concrete have used the strength property of the material. However, high-strength concrete may possess other characteristics that could be used advantageously in concrete structures. Manning (33) suggested that the relationship between high-strength concrete and high-quality concrete may make high-strength concrete attractive not for its strength but for its long-term service performance. The potential for using thin plates of high-strength concrete fabricated on flat beds in the customary manner of the precast concrete industry was reported to be advantageous in the construction of hollow piers for highway bridges (16). Field placement of high-strength, low permeability silica fume added concrete were used as bridge overlay was also reported (10).

Long-span bridges are another area where the qualities of high-strength concrete are proving themselves economically attractive. With greater compressive strength per unit weight and unit volume, high-strength concrete allows lighter and more slender pier structures. In addition increased tensile strength of high-strength concrete is helpful in service load design in prestressed concrete.

Information of some actual buildings and bridges built with high-strength concrete of compressive strength up to 11,000 psi from 1965 to

1984 were compiled in Table 8.1 and Table 8.2 of the ACI committee 363 report (3).

CHAPTER III

EXPERIMENTAL PROGRAM

3.1 Introduction

To carry out the objectives of the research as stated in Chapter I, the experimental program was divided into two parts: the design and construction of the testing facilities; and testing of specimens to evaluate the influence of the parameters including concrete strength, aggregate quality, and crack width opening.

This report deals primarily with the first part of the program, a limited number of preliminary tests needed to evaluate the performance of the testing apparatus are considered.

3.2 Testing Facilities

3.2.1 General

For this research it was necessary to develop equipment to apply a known magnitude of fully reversed cyclic shear force across an open crack in a pavement joint specimen. In addition, suitable instrumentation must be provided to monitor deterioration of the joint resulting from loading. Two test setups were constructed. In both setups loads were applied to specimens by a 50-kip servo-controlled actuator. The suitability of the testing facility was evaluated from several standpoints. At the beginning of a test a suitable crack must be formed in a

specimen at the desired location; the width of the crack must be adjusted to the desired value; and during the application of simulated traffic loads, the equipment must maintain the preset crack width. In addition the loading and data acquisition equipment must function reliably and be functionally compatible.

A typical test specimen, representing an element of an unreinforced concrete pavement slab is shown in Fig. 10. Each specimen, 8.5 by 16 by 36 in., was cast in one piece. To facilitate handling of the specimens, four 1/2-in. bolts were embedded in each end of the specimens. Two planes of weakness were created in the specimens by cutting a groove around the perimeter of a specimen 12 in. from each end. The depths of the grooves were 0.75 in. deep at the top and the bottom faces and 1 in. deep at the side faces. These grooves resulted in a net region for shear transfer of 7 in. by 14 in. The 7-in. depth is comparable to the effective depth at a transverse contraction joint for a 10-in. thick highway concrete pavement.

3.2.2 Initial Test Setup

The general arrangement of the initial test setup is illustrated in Fig. 11. The left and right ends of the specimen were clamped to two MC18x58 channels using four 1-in. steel rods at each end. A fixed support was provided at the left end of the specimen, while a roller support was provided at the right end of the specimen. The middle region of the specimen was clamped by plates which were connected to the loading system. High-strength gypsum cement grout was placed at the interfaces of the specimen and the various steel plates. Steel plates bolted to both ends of the specimen were connected to two 1 in. diameter

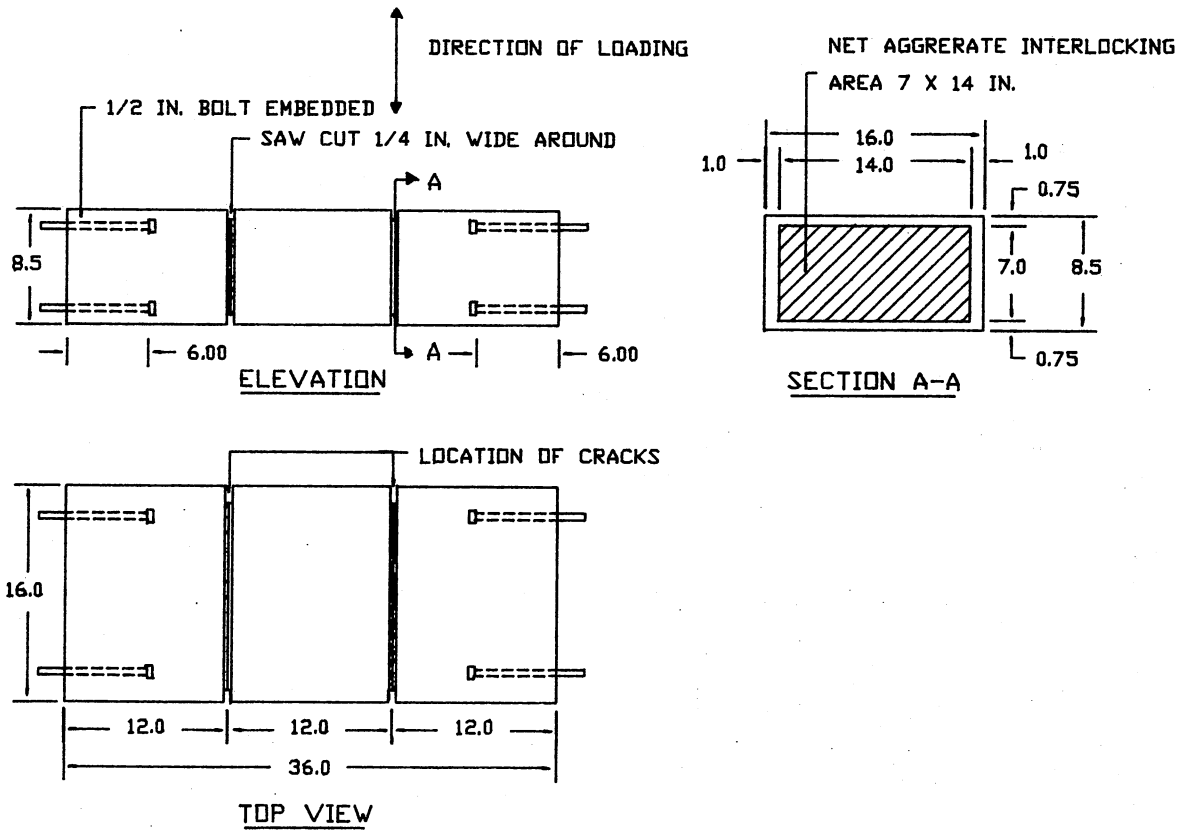

Figure 10. Typical Test Specimen

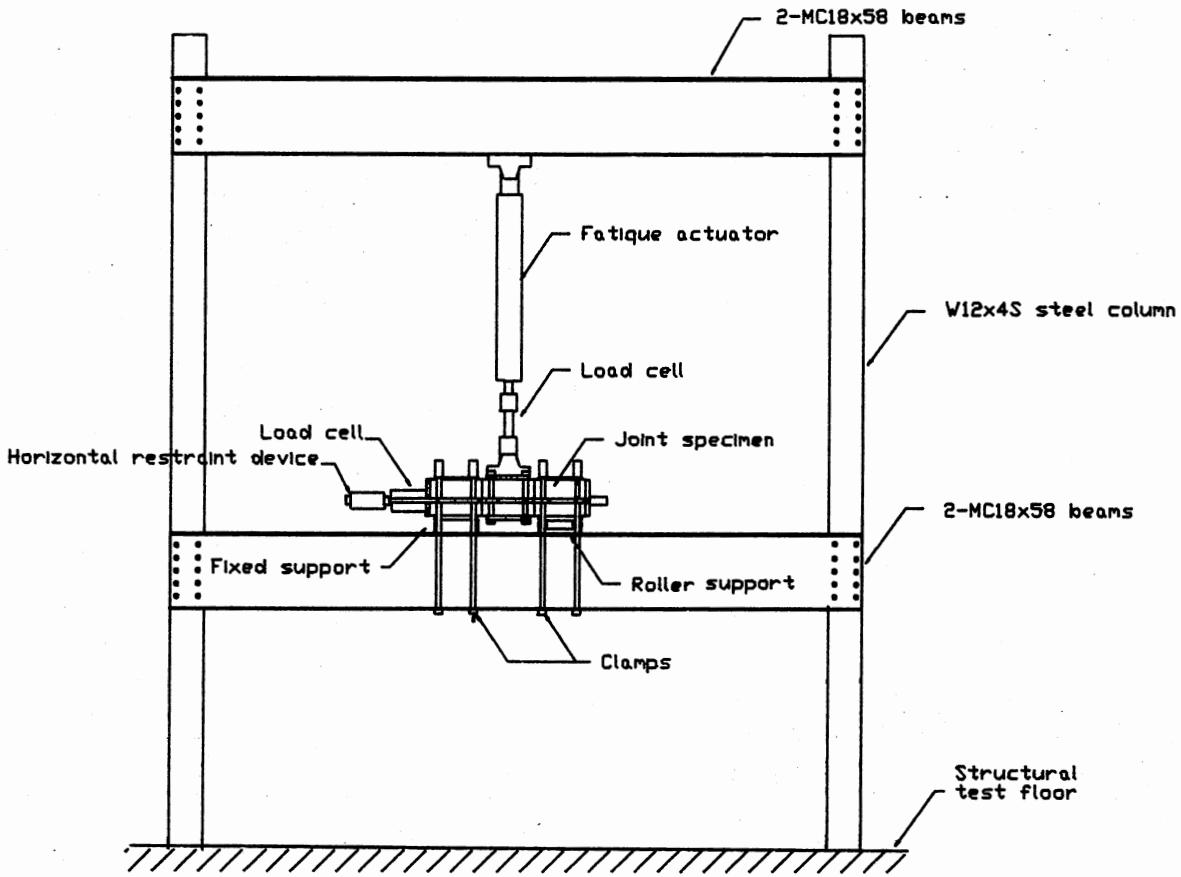

Figure 11. General Arrangement of the Initial Test Setup

threaded steel rods. These rods provided restraint normal to the shear surfaces and by adjusting the position of nuts on the threaded rods, it was possible to set the desired crack width. A load cell used to measure the restraining force was located at one end of the specimen.

Three different methods of forming cracks at the planes of weakness were evaluated. The first method consisted of driving a wedge into the saw kerf. While this method worked on a small prototype specimen, it only produced spalling on the full size specimen. The second and third methods used flexure to crack the specimen. For the second method, the specimen was supported by a pin near the free end and by a roller near the second saw kerf from the supported end and loaded as shown in Fig. 12.

Although not shown in the figure, the horizontal restraining device was attached to the specimen to prevent excessive separation of the crack. After the crack had initiated and propagated through about two-thirds of the depth of the specimen, wedges were inserted in the saw kerf to force the crack to extend across the entire section. This method was then repeated at the other plane of weakness.

For the third method, the specimen was clamped to the supports at both ends, and a hydraulic ram was used to push upward on the supporting channels as shown in Fig. 13. Since the specimen was attached to supports which were fixed to the upper flanges of the channel sections, the action produced negative moment in both the channels and the specimen. Using this method, it was difficult to produce a crack simultaneously at both planes of weakness. Even after cracks had been formed, the actual crack widths were not equal at the two kerfs.

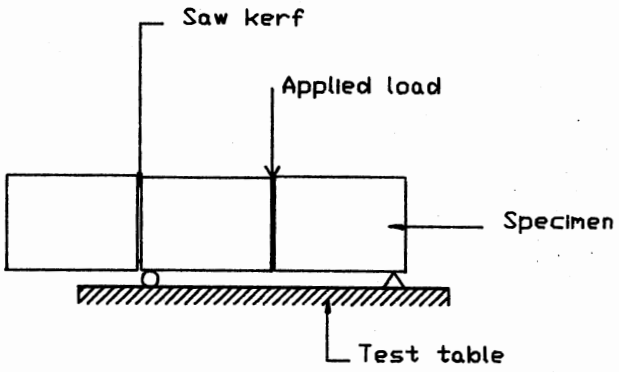

Figure 12. The Second Method of Forming Crack

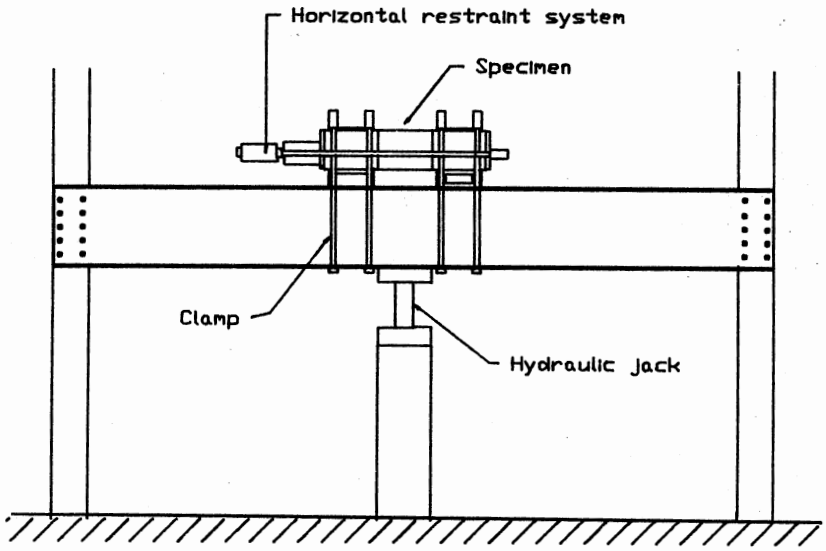

Figure 13. The Third Method of Formimg Crack

In preliminary performance tests using this setup, it was found that the center segment did not assume an average position between the end segments and did not translate vertically. At the top or bottom of one of the joints, the crack width remained quite small. This location, therefore, acted somewhat like a hinge. Consequently, the crack width was too wide at the other joint and loads produced significant rotation rather than translation at the joints. Information obtained from this setup was used in the design of the final test setup.

3.2.3 Final Test Setup

The general arrangement of the final and present test setup is illustrated in Fig. 14. A rigid reinforced concrete reaction frame was constructed and bolted to a structural test floor. Some members of the original loading frame were retained and used to support the actuator. As described above, saw kerfs were placed in the specimen to form planes of weakness at the third-points of the specimen. As shown, the central segment of the specimen was clamped to the concrete reaction frame. The left segment was not in contact with either the reaction frame or load apparatus. The right segment was clamped between plates which were attached to the actuator. The specimen was positioned such that the line of action of the applied load was through the plane of weakness. As before, high strength gypsum cement grout was placed between the specimen and the steel plates before bolts were tightened. The right hand segment of the specimen was restrained normal to the joint surface by a system of linkages which were connected between the steel plates and load cells bolted to the reaction frame. Two load cells were used with the upper linkage, and one load cell was used with the lower linkage.

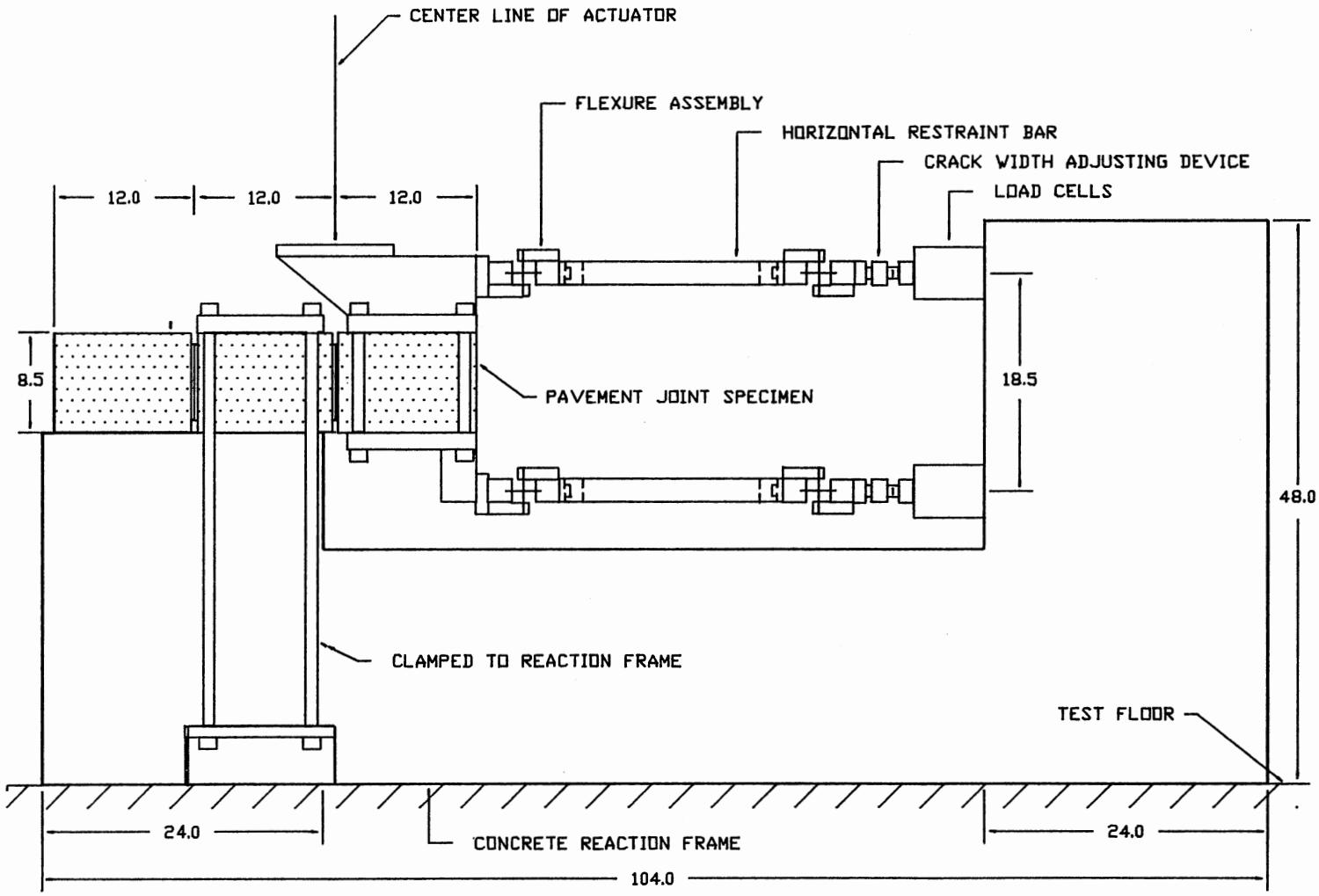

Figure 14a. Elevation View of the Final Test Setup

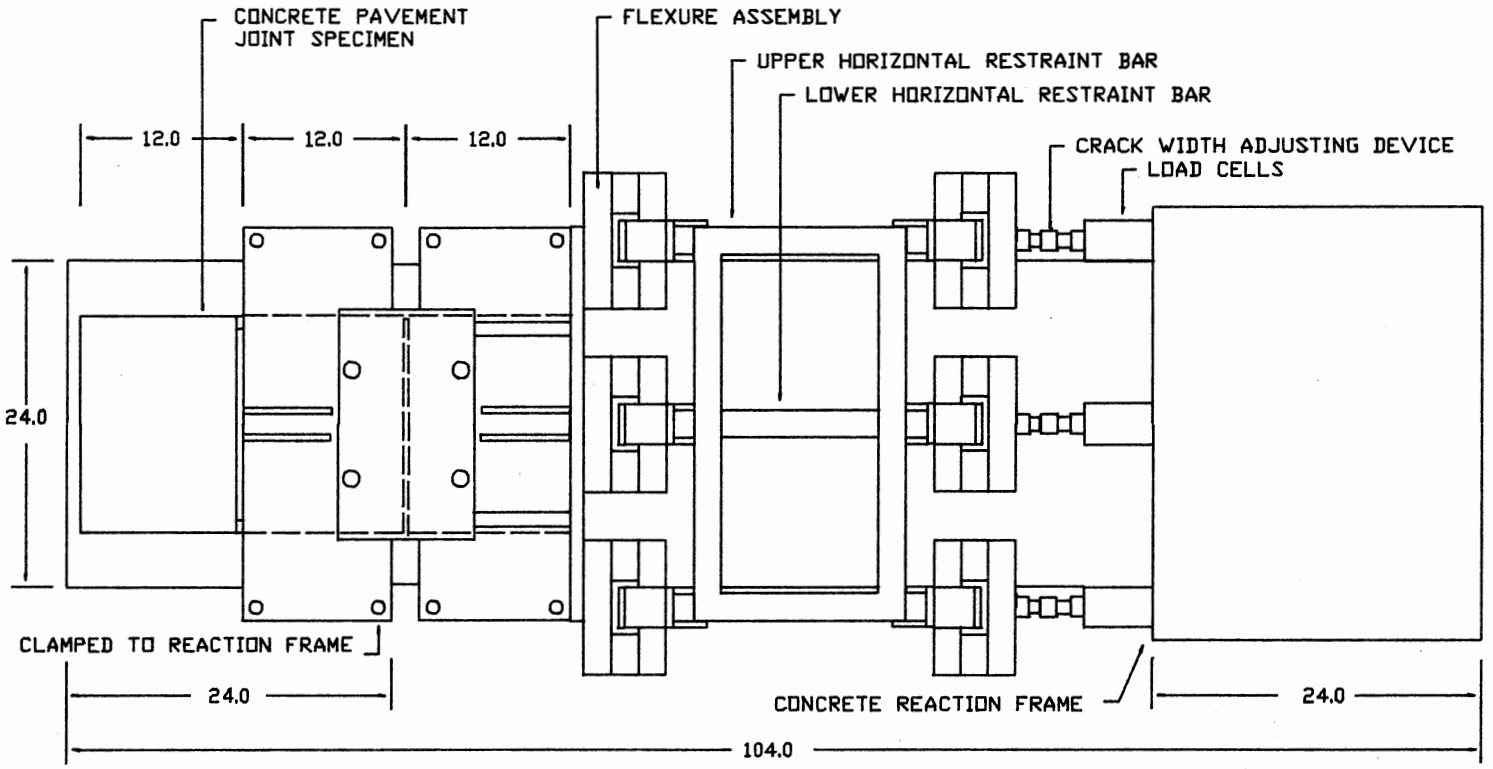

Figure 14b. Plan View of the Final Test Setup

Flexural devices were located at either end of the restraint assemblies. After the specimen was securely clamped into the test fixture and the grout had hardened, a crack was formed by using a hydraulic ram to apply an eccentric force to brackets welded to the upper steel plates. As shown in Fig. 15, a bolt was placed between the brackets and through the center of the hydraulic ram. This bolt was used to control the release of energy as the crack formed.

A turnbuckle-like device was used at each load cell to adjust the crack width of the pavement joint. Figure 16a illustrates the first version of the crack width adjusting device. This device was used together with a rod end in place of the flexural assembly. The present device is shown in Fig. 16b. As can be seen, the stud that threads into the flexural device has a pitch of 8 threads per inch while the stud that threads into the load cell has a pitch of 14 threads per inch. Because of the difference in pitch, one turn of the turnbuckle device shortens or lengthens the linkgage approximately 0.054 in.

3.3 Instrumentation and Data Acquisition System

A view of some of the major items of instrumentation is provided in Fig. 17. The servo-controlled loading system was equipped with three channels of control: load, position and strain. The position channel was used during the installation of test specimens in the test fixture while the load channel was used during the actual testing. A sinusoidal command signal of the desired frequency was supplied by a digital function generator. A load cell attached between the actuator and the specimen was used to measure the applied loads. The magnitude of the applied load was balanced to include the weight of the portion of the

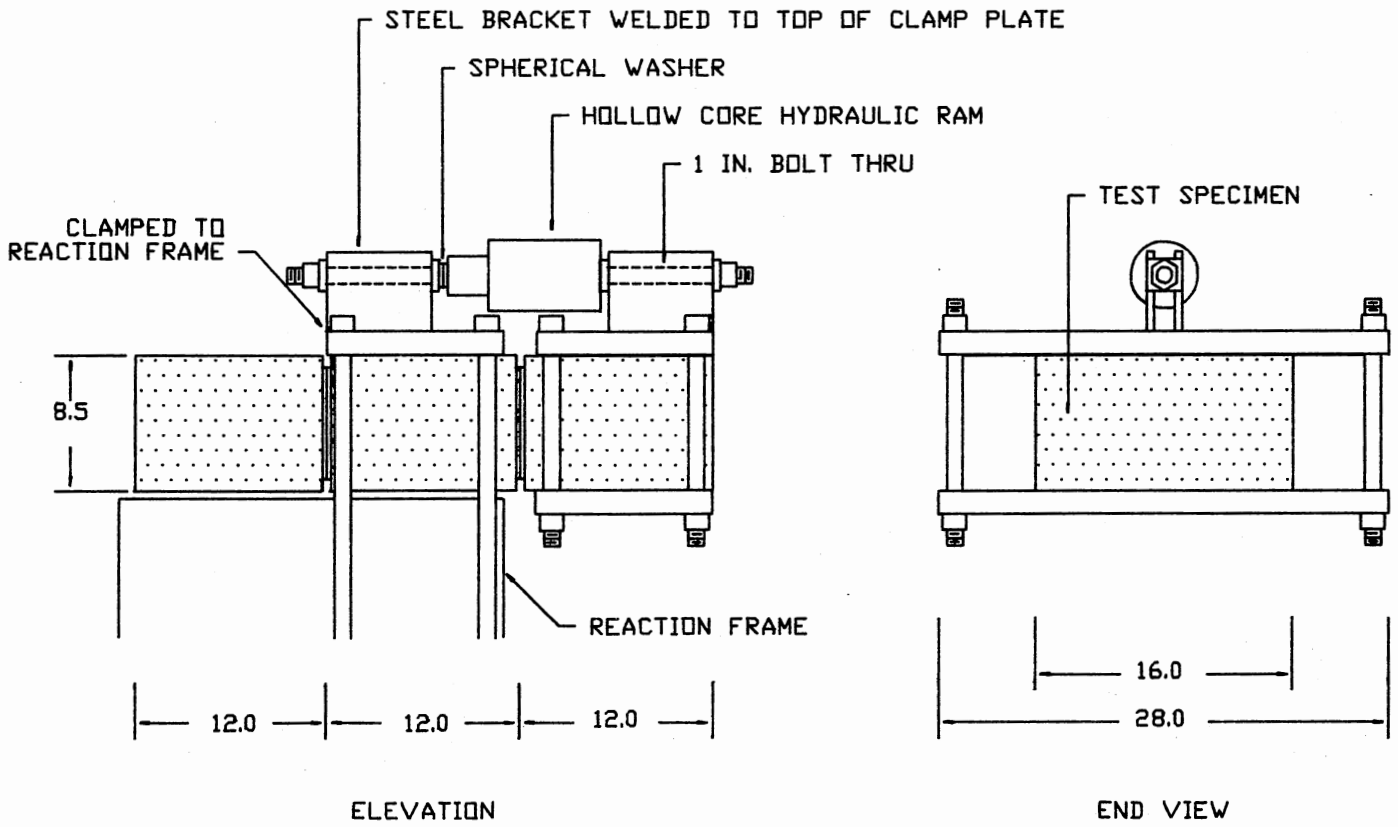

Figure 15. Setup for Forming Crack

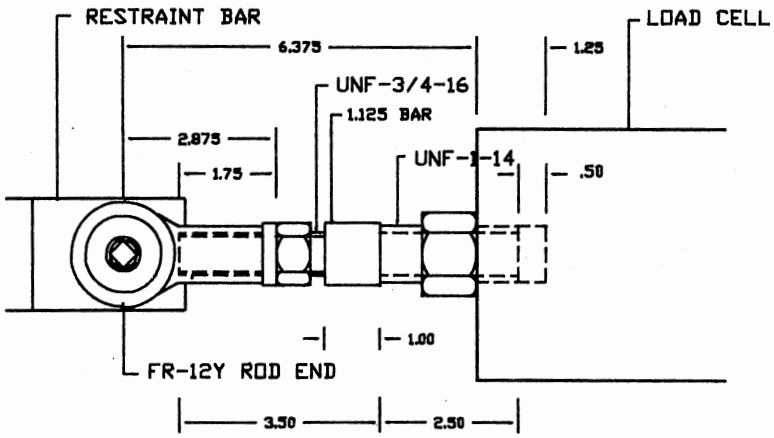

a) Initial Crack Width Adjusting Device

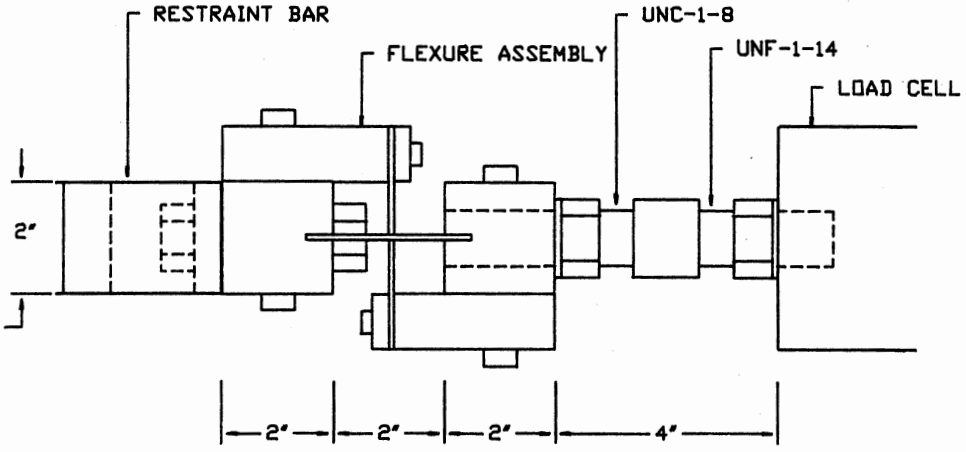

b) Present Crack Width Adjusting Device

Figure 16. Crack Width Adjusting Device

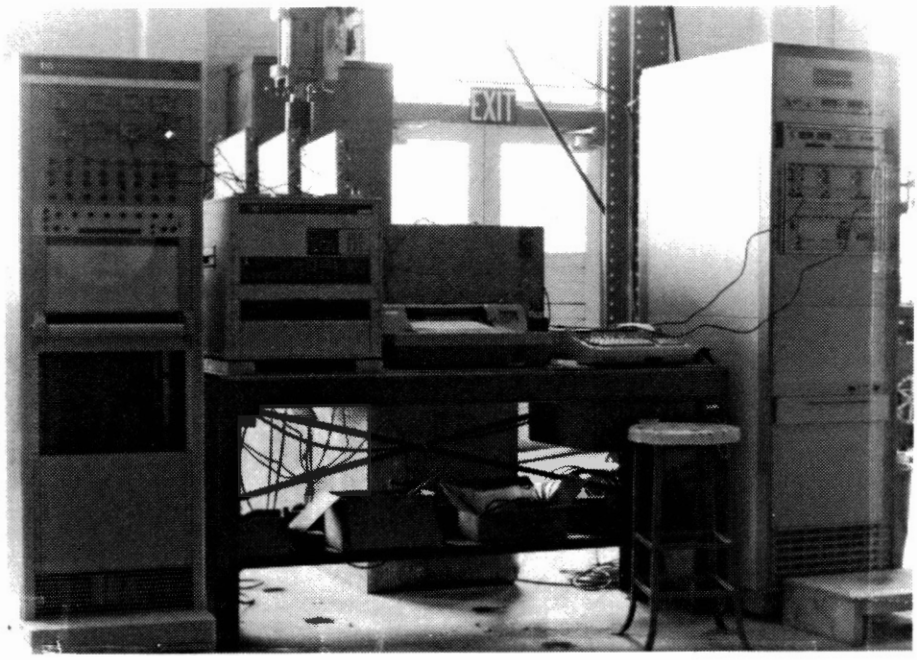

Figure 17. Instrumentation Setup

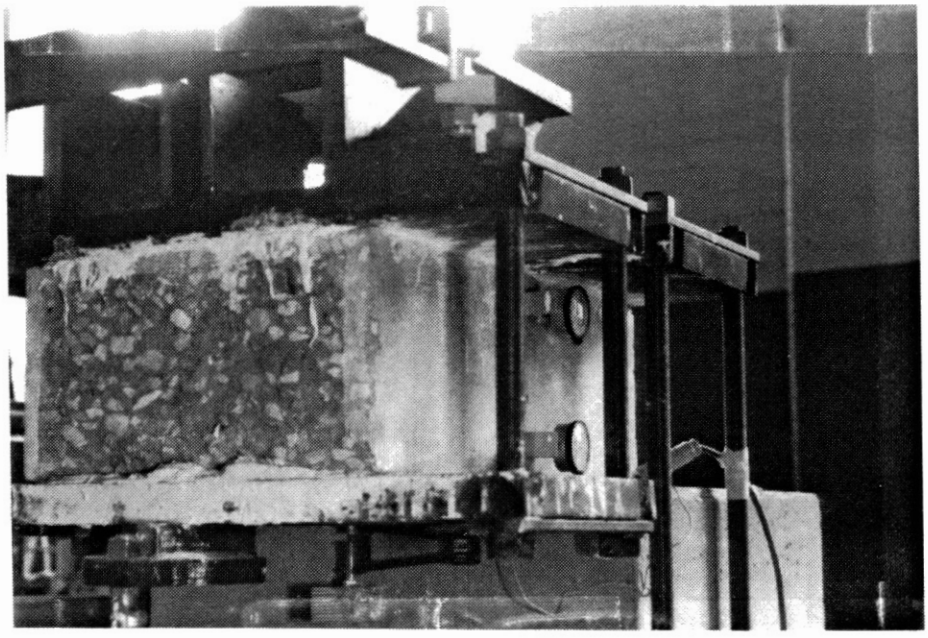

Figure 18. Mounting Arrangement of Gages

specimen and fixtures which attached to the actuator. The strain channel was connected to a clip gage and used to monitor vertical displacement at the pavement joint. The crack width was set and then monitored by four mechanical dial gages with a sensitivity of 0.001 in. per division. The mounting arrangement of the dial gages and the clip gage is shown in Fig. 18. A load cell attached between the actuator and the specimen was used to measure the applied loads. Horizontal restraining forces were measured separately by three 10-kip load cells installed between the ends of the linkgage system and the concrete reaction frame.

A schematic of the computerized data acquisition system developed for the test program is shown in Fig. 19. A scanner and a high speed digital voltmeter were used to measure both the command/feedback voltage from the load channel and the feedback voltage from the strain channel. Outputs from the three load cells measuring horizontal restraining forces were amplified and fed into an HP 7090A Measurement Plotting System. This device had the capability to simultaneously sample the three load cell signals and store 1000 digital voltage readings from each channel in an internal memory buffer. The scanner/voltmeter and the Measurement Plotting System were controlled by an HP 9825 computer. The following data were processed and recorded on tape: 1) the maximum and minimum applied shear forces; 2) the maximum and minimum of the vertical deflections of the joint; 3) the maximum horizontal restraining force at each load cell for each half cycle; and 4) the maximum total restraining force and its location for each half cycle of loading. Data were taken at cycle 1, 10, 100, 1000 and every 1000th cycle thereafter. For monitoring purposes, selected data were displayed graphically by a

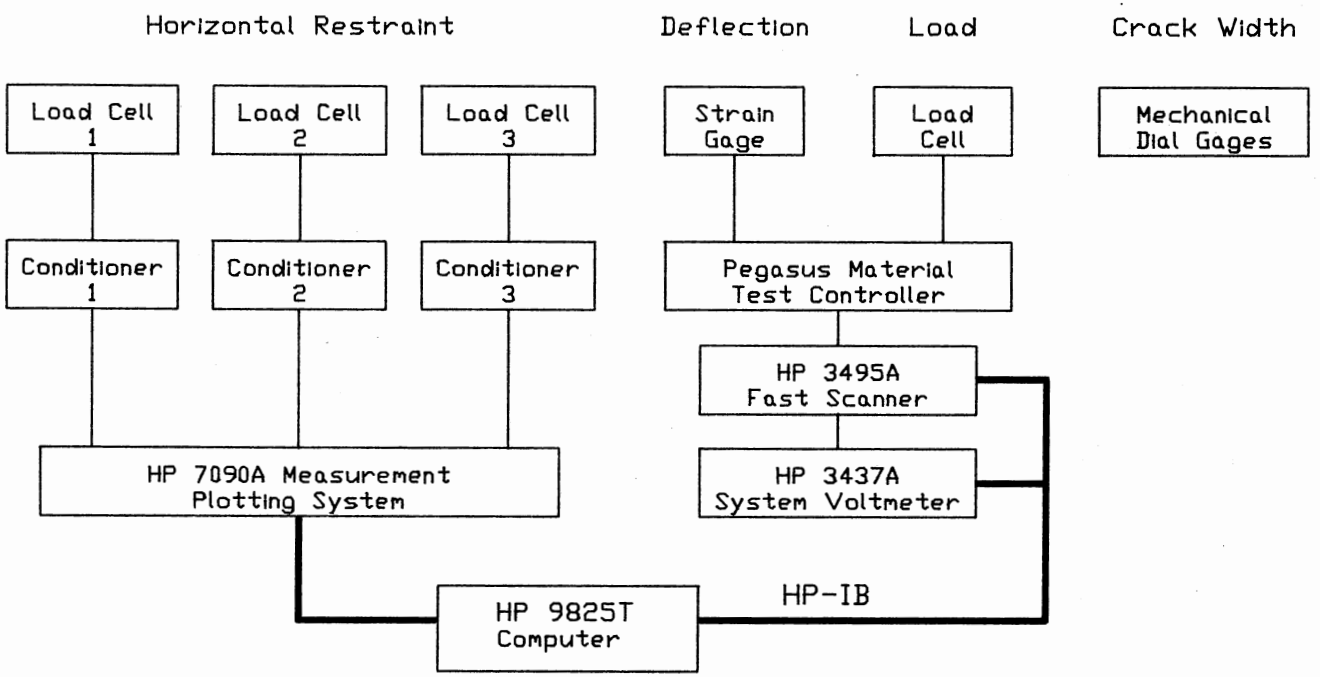

Figure 19. Schematic of Instrumentation

plotter throughout the test.

3.4 Test Specimens

Six specimens were cast in two series, A and H. Each series consisted of three specimens. Specimens were numbered for each series, followed by number 1 or 2 behind a slash indicating the first or the second joint of the specimens. The concrete was made from Type I portland cement and 1 1/2 in. maximum size aggregate. Fly ash Type C of 20% of total cementitious material by weight was used in mix series H. Concrete mix proportions and properties for each series are given in Table III.

TABLE III

MIX PROPORTIONS AND PROPERTIES OF SPECIMENS

Specimen series	H	A
Proportion lb/cu.yd		
Water	270	248
Cement	752	564
Fly ash	188	-
C.A. Size No. 57	1828	1828
Sand	864	1239
Admixtures/100 lb.C		
AEA dos.,ml	40	30
Superplasticizer,fl.oz	9	-
W/C ratio	0.29	0.44
Properties		
Slump,in	2.5	2.5
Air,%	5.3	4.5
Unit Wt.,lb/cu.ft	145	146
28-day strength,ksi	6.41	5.04

The concrete for each specimen was mixed in a single batch using a rotating pan and paddle type mixer with a capacity of 3.75 cu.ft. The fine aggregates were kept moist to prevent segregation. Coarse aggregate was weighed in an air dry condition and then soaked for 24 hours before mixing. Prior to mixing, a sample of sand was oven dried and water was decanted from the coarse aggregate which was again weighed in order to determine the free water added to the mix.

For each batch, the coarse aggregate and fine aggregate were added first to the mix, followed by one-half of the water and admixtures, followed by the cement and fly ash and the remaining water. The mixer was operated for 3 minutes, stopped for 3 minutes and operated again for 2 additional minutes.

Specimens were consolidated in a plywood form using vibration. After finishing, the specimens were covered with plastic. After 24 hours, specimens were removed from the form and were cured under wet burlap covered with polyethylene sheets for 13 days. The specimens were then stored in air until the time of test. Companion compression cylinders were cured in a moist room from the time of casting until they were tested at 28 days.

3.5 Magnitude and Number of Cycles of Loading

It has been shown that joint degradation is negligible at shear stresses of less than 30 psi but is significant at shear stress of approximately 40 psi (8). Therefore, it was decided that a shear stress magnitude of 40 psi would be appropriate for the current investigation. The shear stress of 40 psi over the effective depth of 7 in. and 12 ft. lane width would be produced by a 40-kip single-axle load. The AASHTO

"Interim Guide for Design of Pavement Structures" (1) states that a 40-kip single-axle load applied over 358,295 cycles has an equivalent effect on the performance of the pavement structures as an 18-kip single-axle load applied over 10,000,000 cycles. The same reference further states that this volume of traffics results in damage to a concrete pavement rated at a serviceability index of 2.5. The current study uses fully reversed cyclic load of 3.92 kip applied to the joint specimen for 400,000 cycles.

3.6 Test Procedures

Prior to the installation of each specimen, the output from the three load cells measuring horizontal forces were set to zero. A specimen was then clamped into testing position. All gages were mounted to brackets and were adjusted for the initial condition.

The data acquisition system was next initialized and the test control system was set for load control mode. Five values were recorded at this point as initial readings: applied load, vertical displacement, and restraining forces at each of the three load cells. The crack was then formed and the crack forming equipment was removed. The initial crack width was set by turning the adjustment device.

The specimen was then ready to be tested. Each test was run continuously at an applied load of $\pm$3.92 kip at the rate of 2.0 Hz. The test was terminated when the vertical displacement was at $\pm$0.15 in. or when the 400,000th cycle was completed.

CHAPTER IV

DISCUSSION AND ANALYSIS OF RESULTS

4.1 Introduction

The following discussion is based on preliminary tests of several specimens. When the test facility is fully function, a specimen will be subjected to the required load history. However, during the phase of research the servo-controlled equipment experienced frequent shut downs because of power surges in the AC power supply. In addition, personnel temporarily halted loading to make adjustments to the test equipment on numerous occasions. With the style of servo-controlled equipment used in this research, there is a brief period during pump start up that accurate control of load is impossible. As a result, it is likely that the specimens were subjected to higher than normal loading any time a test was interrupted and the pump was restarted.

4.2 Crack Formation

During preliminary tests all specimens were fully cured prior to the formation of a crack. It was easy to place the uncracked specimen in the test fixtures, apply dial gages to measure crack width and crack the specimen as described earlier. When tests are conducted on specimens which are cracked at an early age and then cured, additional procedures will be needed to be developed to monitor crack width and to per-

mit the handling and installation of specimens.

Because of the random nature of crack formation, each crack surface is unique. For purposes of this research it is necessary that all crack surfaces be essentially plane and perpendicular to the longitudinal axis of the specimen. To obtain this condition it was necessary to place a saw kerf completely around the specimen. Fig. 20 shows a typical crack surface. Because the specimens were fully cured before crack forming, it was observed that the cracks were through the aggregates for all specimens.

The initial system used to provide horizontal restraint involves special rod end bearings. These devices had several thousandths of an inch of 'play' which somewhat complicated the adjustment of the initial crack width. Before crack formation the restraint system was adjusted so that all load cells indicated no load; after crack formation but before application of cyclic load there was a residual crack width and a significant horizontal load sensed by the load cells. Because of the flexibility of the initial restraint system, it was not possible to adjust the crack width to the desired value until cyclic load was applied. For example, when six cycles of load were applied to specimen H 2/1, the width of the crack decreased from 0.021 in. to 0.011 in.

4.3 Horizontal Restraint and Crack Width Control

Use of the turnbuckles to control crack width was found to be satisfactory. During the application of cyclic loads, it was possible to adjust the width of the joint within 0.001 in.

The construction of the horizontal restraint system allowed the

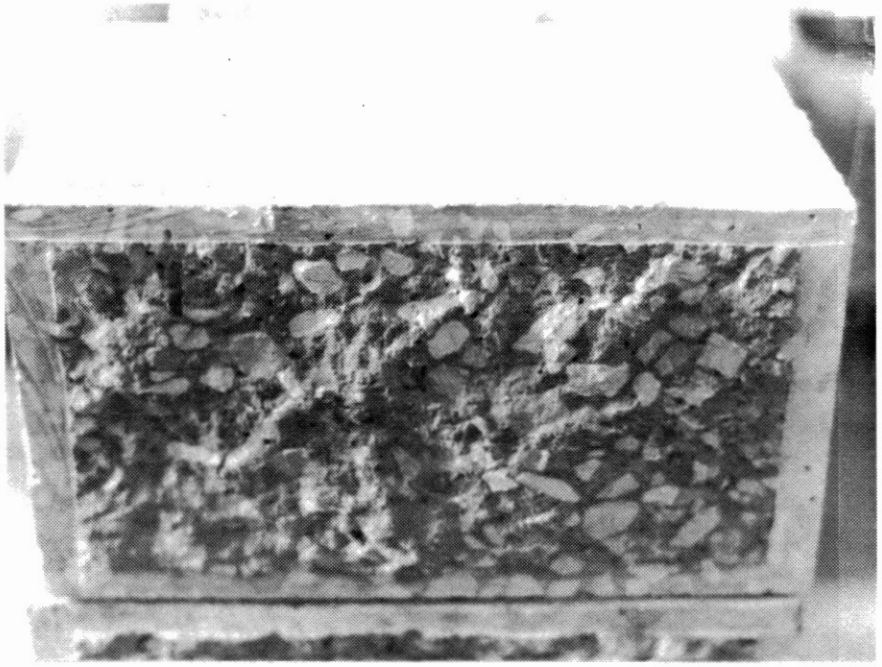

Figure 20. Typical Cracked Surface

specimen to rotate around its longitudinal axis as well as to translate vertically. Because of the rough surfaces of the joint, the rotation of the specimen during load application would permit more contact area of shear transfer which resulted in less localization of shear stresses at the joint than if only vertical translation is allowed.

For specimens with small crack width, initial construction of the linkage system involving the rod end bearings was found to be effective. Specimen A 1/2 was set at 0.014 in. After 10,000 cycles of loads were applied, it was found that the crack width decreased from 0.014 in. to 0.010 in. After resetting the crack width to 0.012 in and continuing loading to 229,000 cycles, the width of the joint increased to 0.015 in. However when the joint was readjusted to a width of 0.014 in., the joint width was maintained at the same readings until cycle 400,000 was reached. Fig. 21 shows the results of specimen A 1/2 test.

Subsequent testing of another specimen A 2/1 at initial crack width of 0.035 in. showed that there was a problem with the horizontal restraining system as it failed to maintain the crack width setting even though the crack width adjusting device was closed to the fullest extent. After only about 50 cycles of loading, The specimen failed severely with several concrete pieces spalling off both the top and the bottom edges of the joint and the vertical displacement reached 0.150 in. which was the limit set for the test.

Specimen A 2/2 was tested at initial joint width of 0.031 in. After 607 cycles of loads were applied, the crack width increased to 0.041 in. The width of the joint continued to increase under the applied loading despite the closing of the crack width adjusting devices. At cycle 887 the joint width was 0.044 in. and increased to 0.067 in. at

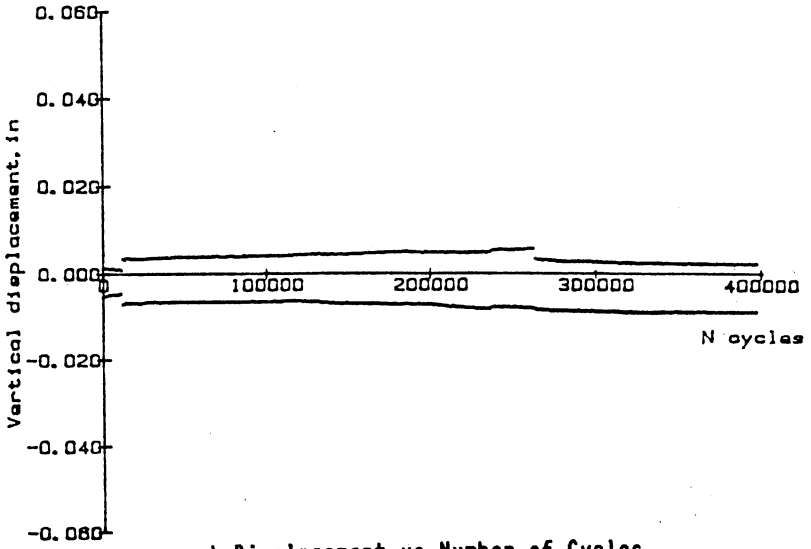

a) Displacement vs Number of Cycles

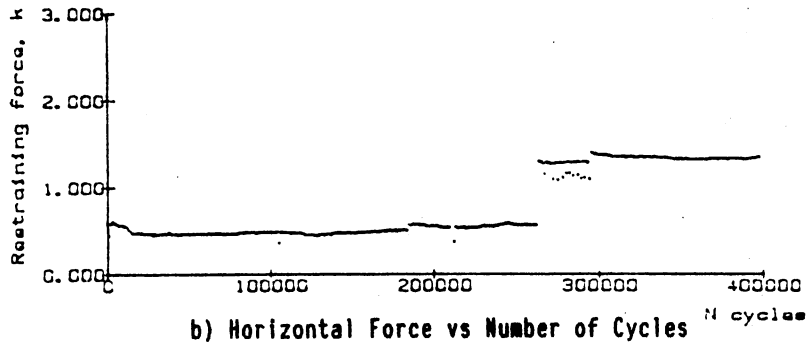

b) Horizontal Force vs Number of Cycles
Upward Loading

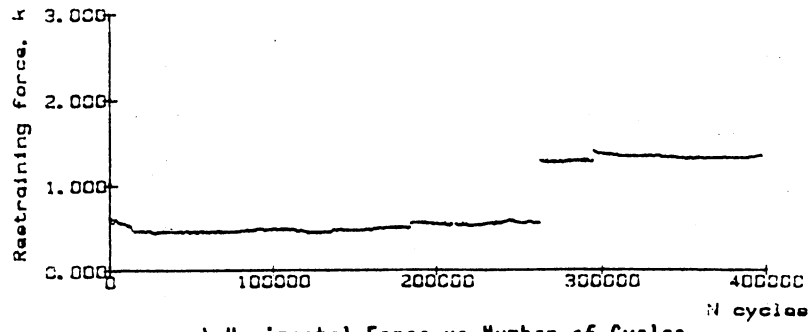

c) Horizontal Force vs Number of Cycles
Downward Loading

Figure 21. Test Results of Specimen A 1/2

cycle 918. The specimen failed at cycle 933 when the vertical displacement reached 0.150 in. and a crack at the bottom edge of the fixed portion of the joint specimen was observed.

Weaknesses of the system were identified at two areas: the flexibility of the connecting straps between the linkage and the rod ends and the sloppiness of the rod end bearings.

An overloading situation occurred caused by a malfunction of a test control panel. The 1/2 in. thick by 2 in. wide steel plates connecting the rod ends to the linkage system were bent. After straightening, they were strengthened by 1/4 in. thick steel plate stiffeners.

After this modification and replacement of the test panel, specimen H 3/2 was tested. At crack width settings of 0.011 and 0.023 in., the linkage system withheld the specimen loading until the test was terminated at cycle 349,000 without failure. The results of this test are shown in Fig. 22. There was a pattern of peaks in the horizontal forces with corresponding dips in vertical displacements encountered at the beginning of the restart of the test after frequent hydraulic pump shutdowns which prevented the test from continuous running. This problem of pump shutdowns was later traced to a defective pump relay. The problem disappeared after the relay was replaced. The overloading might have also damaged the rod end bearings because difficulty in crack width setting was found in this test. Frequent adjustments in crack width were required up to cycle 4390 when the width of the joint became stabilized at a joint width of 0.015 in. With frequent closing of the joint width adjusting devices, the maximum joint width was maintained at 0.015 in. up to cycle 307,000. At this cycle the specimen was reset to a maximum crack width of 0.023 in. The effect of the crack width on the

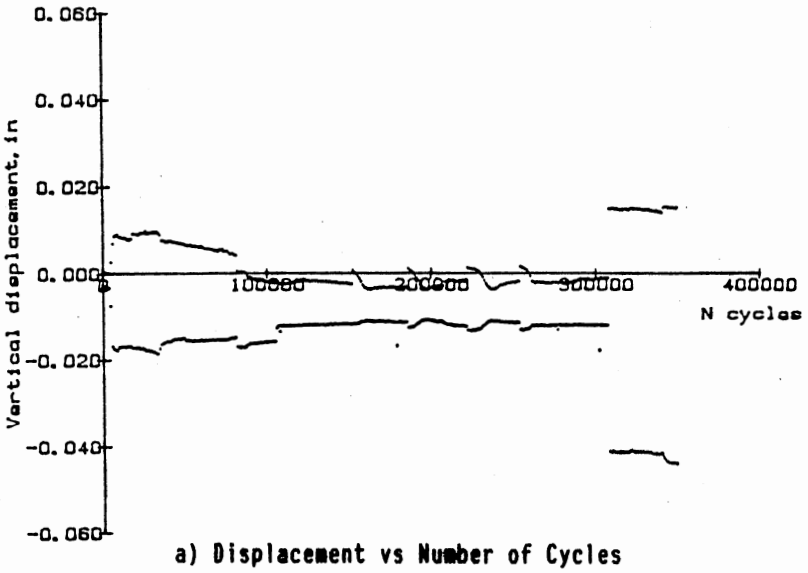

a) Displacement vs Number of Cycles

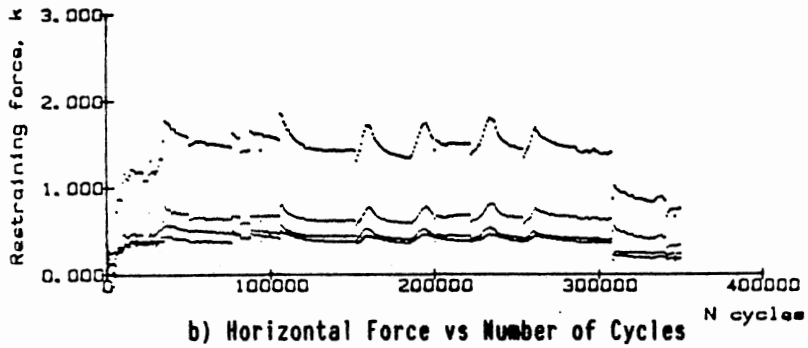

b) Horizontal Force vs Number of Cycles
Upward Loading

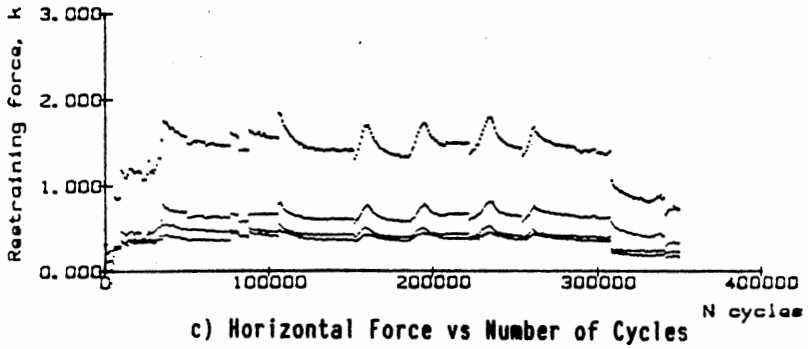

c) Horizontal Force vs Number of Cycles
Downward Loading

Figure 22. Test Results of Specimen H 3/2

shear transfer was seen by the increase in shear displacement (Fig. 22a). This joint width was maintained until cycle 349,000.

The restraining system along with the joint width control device was calibrated for system stiffness. The setup for the calibration is illustrated in Fig. 23. By using position control, a portion of a specimen was held by the actuator. The other portion of the specimen was removed to free the set up from any shear loading. Forces were applied at the centroid of the specimen by a turnbuckle system which had one end connected to the middle of a steel plate bolted to the end of the specimen and the other end anchored to the reaction frame. The load was applied incrementally by turning the turnbuckle. Reaction forces exerted by the restraint system were measured by the three load cells. Horizontal translation of the restraint system was measured by dial gages at four locations on the clamp plates. An additional dial gage was used to detect slippage between the clamp plates and specimen.

Results of the calibration test showed that the sloppiness of the rod end bearings was 0.005 in. and 0.013 in. for upper and lower linkage respectively. Average stiffness of the upper linkage was 89.7 kip/in. and the lower linkage was 62.5 kip/in. This demonstrates that the initial system is too flexible to provide adequate restraint for constant joint width test program. Therefore, modifications of linkage hinges was necessary in order to maintain constant joint width during tests.

Results of the calibration of the present restraining system are shown in Fig. 24. No sloppiness in the flexure assemblies was detected. Average stiffness of the upper linkage was 392 kip/in. and the lower linkage was 261 kip/in. With the present restraint stiffness, if the horizontal reaction at the centroid of the shear surfaces increases by 1

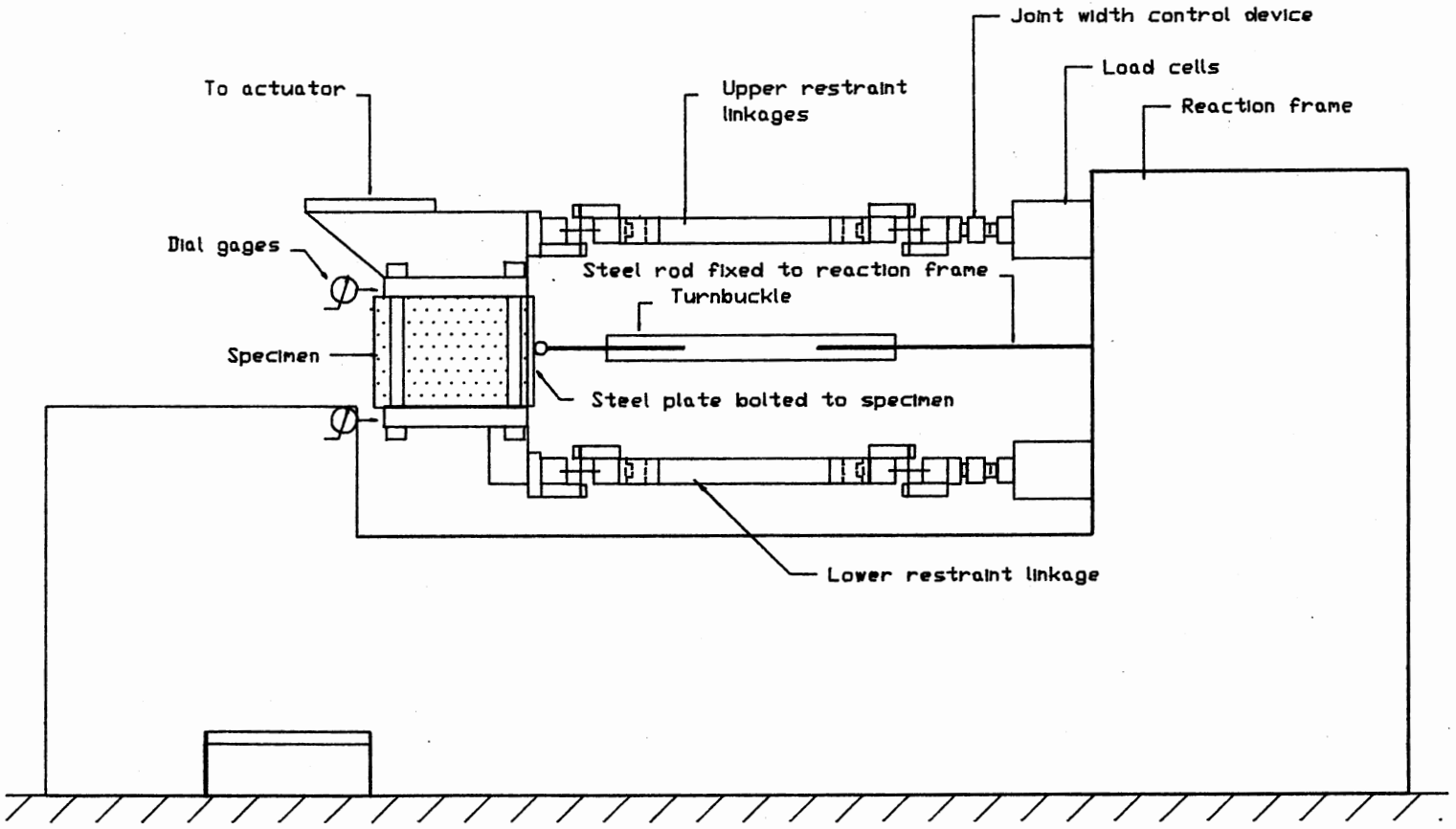

Figure 23. Setup for Restraint System Calibration

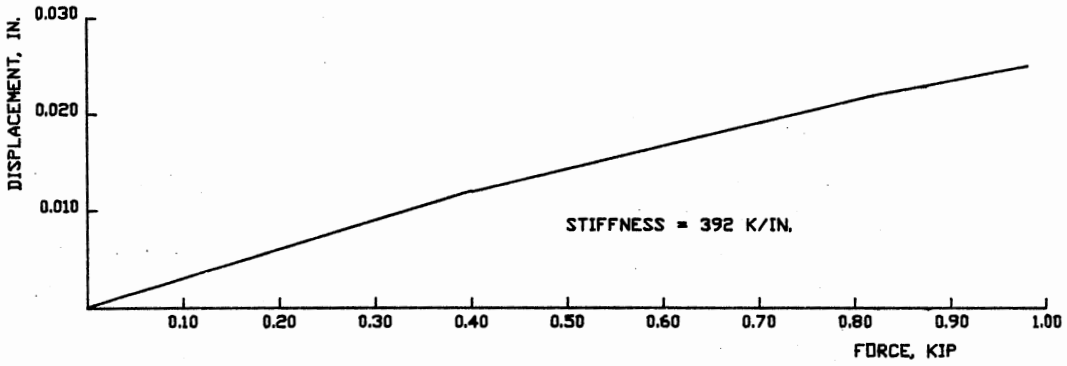

a) Force-Displacement Curve for Upper Linkage

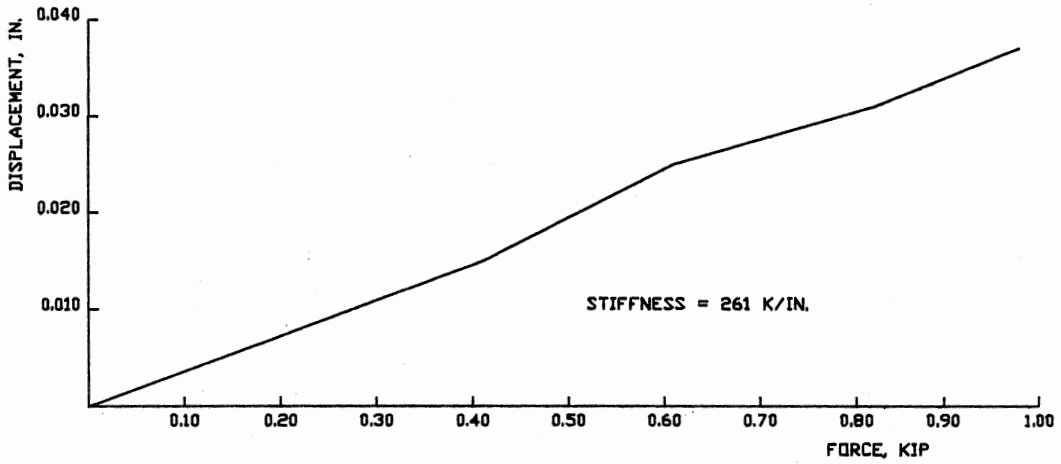

b) Force-Displacement Curve for Lower Linkage

Figure 24. Results of Restraint System Calibration

kip, the width of the crack will increase by approximately 0.001 in. and 0.002 in. at the top and the bottom of the joint respectively.

4.4 Loading Equipment

During the initial check-up of the equipment, problems were encountered with test control panels and hydraulic pump which necessitated repair. However, after all components were reinstalled in full functioning condition, performance of the loading system was quite satisfactory in terms of operation and response.

The load control was selected to operate at 5 kip range full scale output of $\pm$10 volts which is in the 10 percent range of the full capacity of the loading actuator. Therefore, the sensitivity of the load channel was 0.500 k/volt.

The strain channel of the Pegasus test control system measuring vertical displacement, was set at 20 percent range full scale output of $\pm$10 volts with a sensitivity of 0.020 in./volt.

4.5 Instrumentation and Data Acquisition System

Use of mechanical dial gages at four locations worked well for the the crack width setting and monitoring. Because the tips of the dial gages were allowed to contact with the reference brackets at all times during testing, wearing of the tips as well as the brackets was observed. However, this problem can be solved simply by holding back the gage tips and letting them come into contact with the reference brackets only when the measurement of crack width is required.

Overall performance of the data acquisition system was quite satisfactory. Two methods of cycle counting were used in the data acquisi-

tion program. The first method counted cycles by using the high speed system voltmeter to monitor the voltage output of the load channel. The other method was used only during the period of data consolidation which required the computer to perform the task and therefore it was not available for the first method of cycle counting. The latter method counted cycles applied by calculating the time difference between the start and the end of data consolidation in seconds and multiplied it by the rate of cycling in Hz. Because the frequency supplied by the digital function generator was very accurate, precision of the cycle count using the second method was obtained.

4.6 General Observations of the Specimen Behavior

Although only a few of the specimens have been tested as summarized in Table IV, some behavioral trends of the joints subjected to fully reversed cyclic loadings can be observed.

1. Vertical displacement and width of the joint both increased under cyclic loading.
2. Vertical displacement increases with increasing initial crack width.
3. Restraint forces increase under cyclic loading.

TABLE IV

SUMMARY OF SPECIMEN TESTS

Specimen no.	initial joint opening, in.	number of cycles
H1,H2	Crack width setting and data acquisition system debugging	
A1/1	Pump problem	
A1/2	0.012	229,000
	0.014	to 400,000
A2/1	0.035	59
A2/2	0.031	933
H3/1	Failed while adjusting joint width	
H3/2	0.015	307,000
	0.023	to 349,000

CHAPTER V

CONCLUSIONS AND SUGGESTIONS FOR FUTURE WORK

5.1 Conclusions

A test system was developed to evaluate the effectiveness of shear transfer at contraction joints in concrete pavement. The system consisted of four parts: 1) a load application system, 2) a restraining and crack width adjusting system, 3) a crack forming facility, and 4) a data acquisition system. Specimens were designed to represent an element of pavement joint and were used in the performance tests of the test system. The performance tests showed that the system functioned satisfactorily and reliably. Because the initial restraint system involved the use of rod end bearings which had several thousandth of an inch of 'play', difficulties in setting of crack width were found. In addition, calibration tests showed that the initial system was too flexible for constant crack width tests. In the present system, the restraint system was modified by using flexure assemblies in stead of the rod ends. Calibration tests showed that the modified system had no sloppiness and had the total restraint stiffness of 653 kip/in. which is approximately four times greater than the initial system.

5.2 Suggestions for Future Work

5.2.1 Immediate Suggestions

Followings are suggestions for immediate work required for the test system.

5.2.1.1 Test Facilities.

1) For improved safety during installation, a simple hoist system should be constructed to aid in the handling of specimens.
2) In order to form cracks before concrete has achieved significant strength, the following provisions should be made:
   a. gage points should be embedded in the specimen either side of a joint at the time of casting. These will be used in conjunction with a mechanical strain gage to set the width of the joint prior to test.
   b. a longitudinal force should be applied to specimens which are cracked at an early age. This force applied by a simple arrangement of threaded rods attached to plates at the end of the specimen will hold the newly fractured surfaces in proper alignment until the specimen is later installed in the test fixture.

5.2.1.2 Test Program.

1) To assess the influence of concrete strength, it is suggested that the test program should cover a range of strength from 4 to 8 ksi.

2) To determine the benefit of high-strength concrete for marginal aggregate, it is suggested that two different aggregates with decreasing degree of abrasion resistance and freeze-thaw durability should be used.
3) The program should include both the constant and variable crack widths tests. For the constant crack width tests, joint width of 0.035, and 0.065 in. are suggested.
4) To determine the influence of the age at cracking, it is suggested that a specimen is cracked at the age of 1 day and 28 days.

5.2.2 Long-Term Suggestions

With the same test facilities, the research should be extended to cover the influence of high-strength concrete with marginal aggregate on the load transfer capability of doweled joints. The width of the specimen can be increased to 24 in. to accommodate two dowels at a normal spacing of 12 in. without any modification to the existing clamping fixtures.

REFERENCES

1. "AASHTO Interim Guide for Design of Pavement Structures." New York, N.Y.: AASHTO, 1981.

2. ACI Committee 325. "Structural Design Considerations for Pavement Joints." Journal of the American Concrete Institute, Vol. 81, No. 1 (July 1956), pp. 1-28.

3. ACI Committee 363. "State-of-the-Art Report on High Strength Concrete." Journal of the American Concrete Institute, Vol. 81, No. 4 (July/August, 1986), pp. 364-411.

4. Anderson, A. R. "Research Answers Needed for Greater Utilization of High Strength Concrete." Journal of the Prestressed Concrete Institute, Vol. 25, No. 4 (July-August, 1960), pp. 162-164.

5. Birkeland, P. W. and Birkeland, H. W. "Connections in Precast Concrete Constructions." Journal of the American Concrete Institute, Vol. 63, No. 3 (March, 1966), pp. 345-368.

6. Blick, R. L., Peterson, C. F., and Winter, M. E. "Proportioning and Controlling High Strength Concrete." American Concrete Institute Special Publication, SP-46 (1974), pp. 141-163.

7. Carrasquillo, R. L., Nilson, A. H., and Slate, F. O. "Microcracking and Behavior of High Strength Concrete Subjected to Short-Term Loads." Journal of the American Concrete Institute, Vol. 78, No. 3 (May-June, 1981), pp. 179-186.

8. Colley, B. E. and Humprey, H. A. "Aggregate Interlock at Joints in Concrete Pavements," Highway Research Record, No. 189 (1967), pp. 1-18.

9. Copen, M. D. "Problems Attending Use of Higher Strength Concrete in Thin Arch Dam." Journal of the American Concrete Institute, Vol. 72, No. 4 (April, 1975), pp. 138-140.

10. "Dense Mix Fights Road Salt," Engineering News-Record, (November 8, 1984), pp. 16.

11. Fattah-Shaikh, A. "Proposed Revisions to Shear-Friction Provisions." Journal of the Precast Concrete Institute, Vol. 23, No. 2 (March/April, 1978), pp. 12-21.

12. Fenwich, R. C. and Paulay, T. "Mechanisms of Shear Resistance of Concrete Beams." Journal of the Structural Division, ASCE, Vol. 94, No. ST10 (October, 1968), pp. 2325-2350.

13. Fardis, M. N. and Buyukotzturk, O. "Shear Transfer Model for Reinforced Concrete," Journal of Engineering Mechanics, ASCE, Vol. 105, No. EM2 (April, 1979), pp. 255-275.

14. Hofbeck, J. A., Ibrahim, I. O., and Mattock, A. H. "Shear Transfer in Reinforced Concrete." Journal of the American Concrete Institute, Vol. 66, No. 2 (February, 1969), pp. 119-128.

15. HRB Special Report 61G "The AASHO Road Test, Report 7, Summary Report," National Academy of Sciences-National Research Council Publication 1061, 1962.

16. Jobse, H. J. and Moustafa, S. E. "Applications of High Strength Concrete for Highway Bridges." Journal of the Precast Concrete Institute, Vol. 29, No. 3 (May/April, 1984), pp. 45-73.

17. Laible, F., White, R. N., and Gergely, P. "An Experimental Investigation of Seismic Shear Transfer Across Cracks in Concrete Nuclear Containment Vessels." American Concrete Institute Special Publication, SP-53-9 (1977), pp. 203-226.

18. Mattock, A. H. and Hawkins, N. M. "Shear Transfer in Reinforced Concrete-Recent Research." Journal of the Precast Concrete Institute, Vol. 17, No. 2 (March/April, 1972), pp. 55-75.

19. Mattock, A. H. "Cyclic Shear Transfer and Type of Interface." Journal of the Structural Division, ASCE, Vol. 107, No. ST10 (October, 1981), pp. 1945-1964.

20. Millard, S. G. and Johnson, R. P. "Shear Transfer Across Cracks in Reinforced Concrete Due to Aggregate Interlock and Dowel Action." Magazine of Concrete Research, Vol. 36, No. 126 (March, 1984), pp. 9-21.

21. Millard, S. G. and Johnson, R. P. "Shear Transfer in Cracked Reinforced Concrete." Magazine of Concrete Research, Vol. 57, No. 130 (March, 1985), pp. 3-15.

22. Mphonde, A. G. and Frantz, G. C. "Shear Tests of High and Low Strength Concrete Beams without Stirrups." Journal of the American Concrete Institute, Vol. 81, No. 4 (July/August, 1984), pp. 350-357.

23. Nowlen, W. J. "Influence of Aggregate Properties on Effectiveness of Interlock Joints in Concrete Pavements." Journal of the PCA Research and Development Labarotary, Vol. 10, No. 2 (May, 1968), pp. 2-8.

24. Paulay, T. and Loeber, P. J. "Shear Transfer by Aggregate Interlock." American Concrete Institute Special Publication, SP-42, "Shear in Reinforced Concrete," Vol. 1 (1974), pp. 1-16.

25. Reinhardt, H. W. and Walraven, J. C. "Cracks in Concrete Subject to Shear." Journal of the Structural Division, ASCE, Vol. 108, No. ST1 (January, 1982), pp. 207-224.

26. Shober, S. F. "Portland Cement Concrete Pavement Performance as Influenced by Sealed and Unsealed Contraction Joints." Transportation Research Record, No. 1083 (1986), pp. 7-12.

27. Swamy, R. N. and Andriopoulos, A. D. "Contribution of Aggregate Interlock and Dowel Forces to the Shear Resistance of Reinforced Beams without Web Reinforcement." American Concrete Institute Special Publication, SP-42, "Shear in Reinforced Concrete," Vol. 1 (1974), pp. 129-166.

28. Taylor, H. P. J. "The Fundamental Behavior of Reinforced Concrete Beams in Bending and Shear." American Concrete Institute Special Publication, SP-42, "Shear in Reinforced Concrete," Vol. 1 (1974), pp. 43-78.

29. Walraven, J. C. "Fundamental Analysis of Aggregate Interlock," Journal of the Structural Division, ASCE, Vol. 107, No. ST11 (November, 1981), pp. 2245-2271.

30. Wang, C. K. and Salmon, C. G. "Reinforced Concrete Design." 4th Ed. Harper and Row, Publishers, New York, (1985).

31. White, R. N. and Holley, M. J. "Experimental Studies of Membrane Shear Transfer." Journal of the Structural Division, ASCE, Vol. 98, No. ST8 (August, 1972), pp. 1835-1852.

32. Wittman, F. H. "Micromechanics of Achieving High Strength and Other Superior Proporties." Proceeding, National Science Foundation Workshop on High Strength Concrete, University of Illinois at Chicago Circle, (December, 1979), pp. 8-30.

33. Young, F. J. and Russel, H. G. "Session V - Summary of Floor Discussion." Proceeding, National Science Foundation Workshop on High Strength Concrete, University of Illinois at Chicago Circle, (December, 1979), pp. 220-222.

APPENDIXES

APPENDIX A

DATA ACQUISITION SYSTEM SOFTWARE MANUALS

A.1 User's Guide Manual

This user's guide covers the data acquisition software for a HEWLETT PACKARD 9825T computer. In addition to the computer, the following equipment is required:

Equipment	Purpose
HP 7090A Measurement Plotting System	Acquire three channels of data and data plotting
HP 3495A Scanner	Multiplex two channels of data to the System Voltmeter
HP 3437A System Voltmeter	Provide high speed data sampling
HP 7245A Plotter/Printer	Provide print outs

1. LOADING THE PROGRAM:

   a) Insert the program tape in the HP 9825T tape drive.

   b) <rew> <execute>

   c) <trk 1>

   d) <ldf 1>

   e) <run>

2. RUNNING THE PROGRAM: When the program is started, the system will display information about the software and its limitations. The user is then prompted for sensitivity, units of sensitivity, and voltage range for each channel. Channel designations are assigned as follows:

Channel	Device	Measurement
1	Scanner channel 0 SVM	Pegasus load channel
2	Scanner channel 1 SVM	Pegasus strain channel
3	HP 7090A channel 1	Upper-north load cell
4	HP 7090A channel 2	Lower-middle load cell
5	HP 7090A channel 3	Upper-south load cell

3. The system will ask whether the user needs an echo print of the input data (responds with 1 for yes or 0 for no). If the user enters 0 for this step, system will skip to step 4. If the response is 1, the system will print sensitivity value, sensitivity unit, and voltage range for all channels.

4. After the echo print is finished, the system will ask the user whether the setup is ok. If everything is correct, the system will go on to the next step. Otherwise, the system will go back to step 1.

5. The prompt, "Record Data?" will appear on the display. If data recording is required, the user must respond with a "1".

The user must then insert a data tape and enter the track number to be used for data storage (two tracks, 0 and 1, are available on each data tape). The system will ask the user if the tape needs to be formatted. For this program, each tape is marked with an initial file of 200 bytes long and 500 files of 150 bytes each. If the user enters 1, the data tape will be automatically formatted by the system.

6. The prompt, "Plot data?" will appear on the display. If the user wants to plot data; he should load paper and pens in the HP 7090A and respond with a "1".

7. The system is now ready for measurements to be started. The prompt, "Record initial reading?" will appear on the display. If the user responds with a "1", these data will be stored in file number 0. NOTE: The user must do this before cracking the specimen. This step is important in case of machine breaks down. If the user wants to restart the machine after the breakdown, the user can answer 0 to skip the recording of initial data.

8. The user can start testing the specimen at this step. The system will monitor the applied load and will keep a cycle count for the test. At cycle 1, 10, 100, and at every 1000th cycle thereafter, the computer will read data from all five channels. If requested (see step 5), these data will be stored on the data tape. If data are recorded onto tape and the starting track is track no. 1, the user must insert a new tape or enter a new track number when the starting track is full. The user will notice this by a system prompt "Track 1 is full: Insert new tape". However, if the starting track is track 0, the system will automatically change to track 1 when track 0 is full.

A.2 Technical Reference Manual

This program is written to allow automated data acquisition during the test of joint specimens. The data acquisition system is composed of a HP 3437A high speed System Voltmeter, HP 3495A Scanner, HP 7090A Measurement Plotting System, HP 7245A Printer/Plotter, and HP 9825T Computer.

The HP 3437A System Voltmeter is a high speed, 3-1/2 digit, dc voltmeter which provides high speed sample of 3.8 msec on three selectable voltage ranges: 10, 1, and 0.1 V. The input multiplexer for the voltmeter is the HP 3495A Scanner. The scanner provides multi-channel closures at a maximum rate of 125 channels per second.

The HP 7090A is a three-channel analog-to-digital data acquisition system and a digital plotter packaged into a single instrument. In the buffer recording mode, it is capable of storing 1,000 samples from each channel in separate buffers at a rate determined by the total time setting (times from 0.03 seconds to 24 hours are allowed). Each buffer is simultaneously filled in the specified time. The stored sample values can subsequently be sent to a computer. The range sensitivity of each channel may be set independently from 5 mV to 100 V full scale.

The HP 9825T computer is used as the System Controller. The controller is integrated with the system's instruments through an HP-IB interface.

Inputs to the data acquisition system are voltage signals from the load and strain channels of the Pegasus Test Control System and three load cells measuring horizontal restraining forces. The specific purpose and select code for each device is listed below:

Equipment	HP-IB select code	Purpose
HP 7090A Measurement Plotting System	707	Acquire three channels of data and data plotting
HP 3495A Scanner	709	Multiplex two channels data to the SVM
HP 3437A System Voltmeter	724	Provide high speed data sampling
HP 7245A Plotter/ Printer	705/706	Provide data listings and/or data plots

The software channel number and the associated device is as follows:

Channel	Device	Measurement
1	Scanner channel 0 SVM	Pegasus load channel
2	Scanner channel 1 SVM	Pegasus strain channel
3	HP 7090A channel 1	Upper-north load cell
4	HP 7090A channel 2	Lower-middle load cell
5	HP 7090A channel 3	Upper-south load cell

Initially, the user must provide values of sensitivity, sensitivity units, and voltage ranges for all 5 channels. The program is written so that the user may have the option of recording experimental data on tape, and/or monitoring data graphically. NOTE: It is important that the user ensures that the hydraulic actuator cycles at 2.0 Hz. The program is written to be used at this rate. The program takes readings of all channels at cycle 1, 10, 100, and every 1000th cycle thereafter.

When the test is started, the program starts monitoring the cycle count by triggering the SVM to read the load voltage sine-wave signal

and compare it to a set voltage level of +1. The comparison continues until the voltage reading passes from a value of less than +1 V to a value of greater than +1 V, which indicates the start of a cycle. The cycle completes when the same condition occurs for a second time.

At the start of cycle 1, the program takes measurement by initiating the HP 7090A (in buffer recording mode with a 5-second period) and calling subroutine 'red' to read 25 voltage signals per cycle each of the load and strain channels. At cycle 10, subroutine 'red' is called a second time to read the measurements. At this time, the HP 7090A (which still continues its buffer recording function) also stores data from the three load cells for cycle 10. There is a check point in the program at this step to ascertain that enough processing time for buffer recording is provided.

When the buffer is filled, subroutine 'buf' is called to transfer data from the buffer to the microcomputer at a rate of 13 readings per cycle. Subroutine 'mon' will be called when the buffer is empty. 'mon' monitors the cycle count and initiates the readings at cycle 100. After the buffer is filled for a second time, subroutine 'consol' is called to consolidate data that have been stored in computer memory. If it is preferred by user, the consolidated data will be recorded on tape and/or will be plotted on the HP 7090A. During this period of consolidation, the cycle count is approximated by calculating the time difference from the start and the end of the consolidation. Subroutine 'time' is called at the start and the end of this period requesting clock time from the HP 7090A. Another subroutine 'count_time' is called to calculate the time difference in seconds. The number of cycles passed during this period is estimated by considering 2 cycles per second.

The updated number of cycles is passed to 'mon', which is called to continue monitoring the cycle count and initiate the readings at the next specified cycle. This process will be repeated at every 1000th cycle until the 400,000th cycle is reached.

The following appendixes include the flow chart for the main program, a detailed description and flow chart of each subroutine, and the complete program listing.

APPENDIX B

PROGRAM FLOW CHARTS

MAIN PROGRAM

'INIT':
* Set no. of channel

'cd':
* S[I] : Sensitivity of channel I
* U$[I]: Sensitivity unit for channel I
* R[I] : Voltage range for channel I

'echo':

'set':

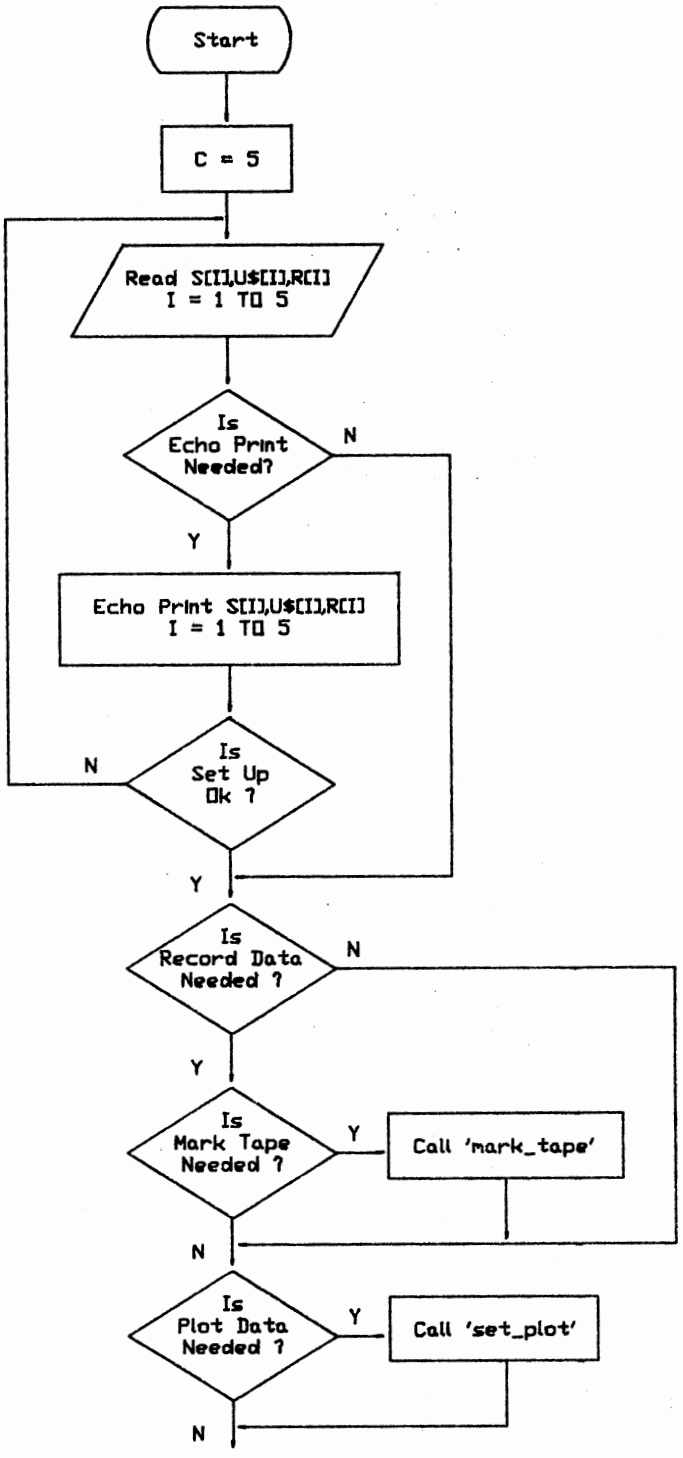

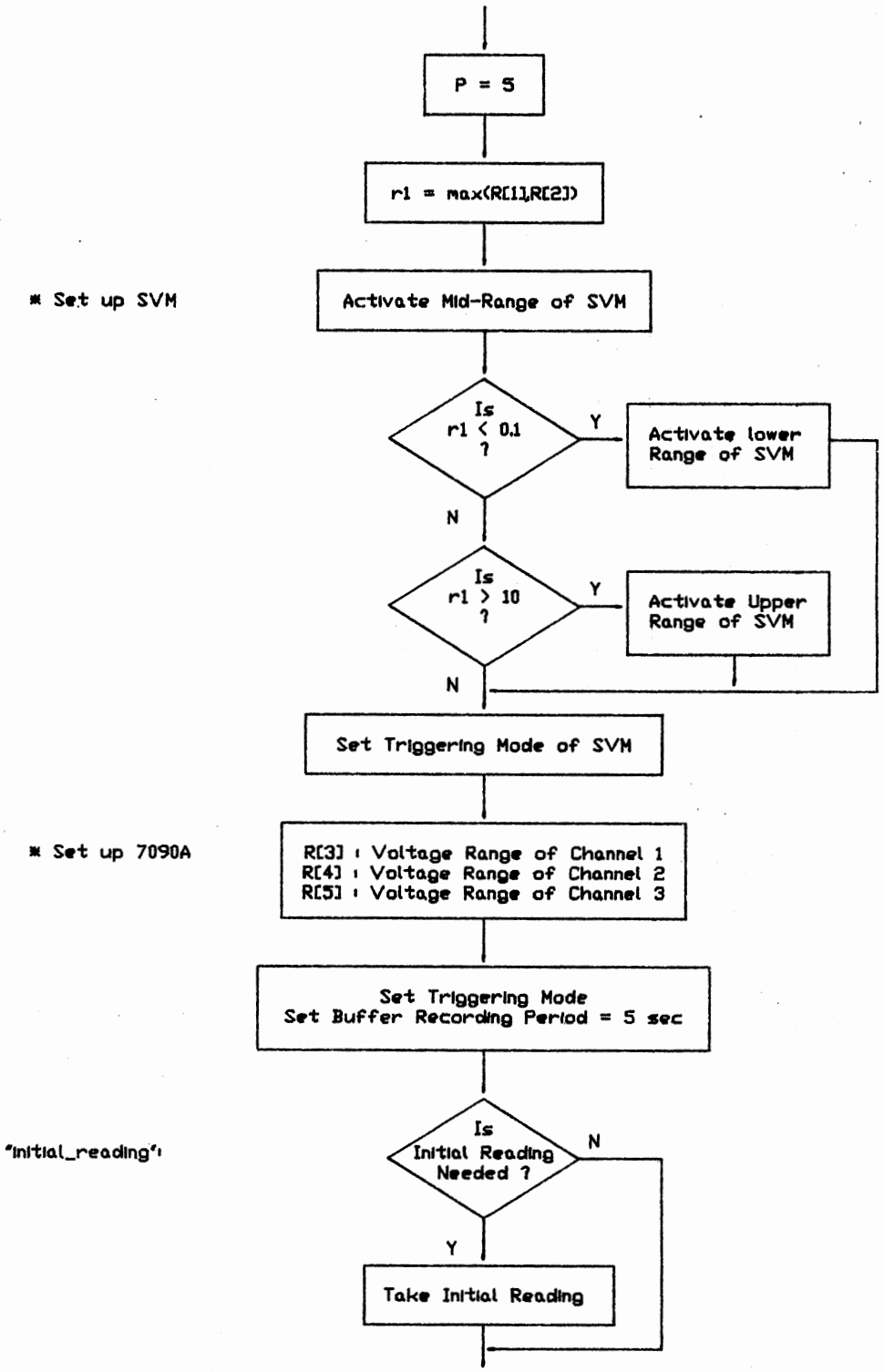
P = 5
r1 = max(R[1],R[2])
* Set up SVM
Activate Mid-Range of SVM
Is r1 < 0.1 ?
Y
Activate lower Range of SVM
N
Is r1 > 10 ?
Y
Activate Upper Range of SVM
N
Set Triggering Mode of SVM
* Set up 7090A
R[3] : Voltage Range of Channel 1
R[4] : Voltage Range of Channel 2
R[5] : Voltage Range of Channel 3
Set Triggering Mode
Set Buffer Recording Period = 5 sec
"Initial_reading"
Is Initial Reading Needed ?
N
Y
Take Initial Reading

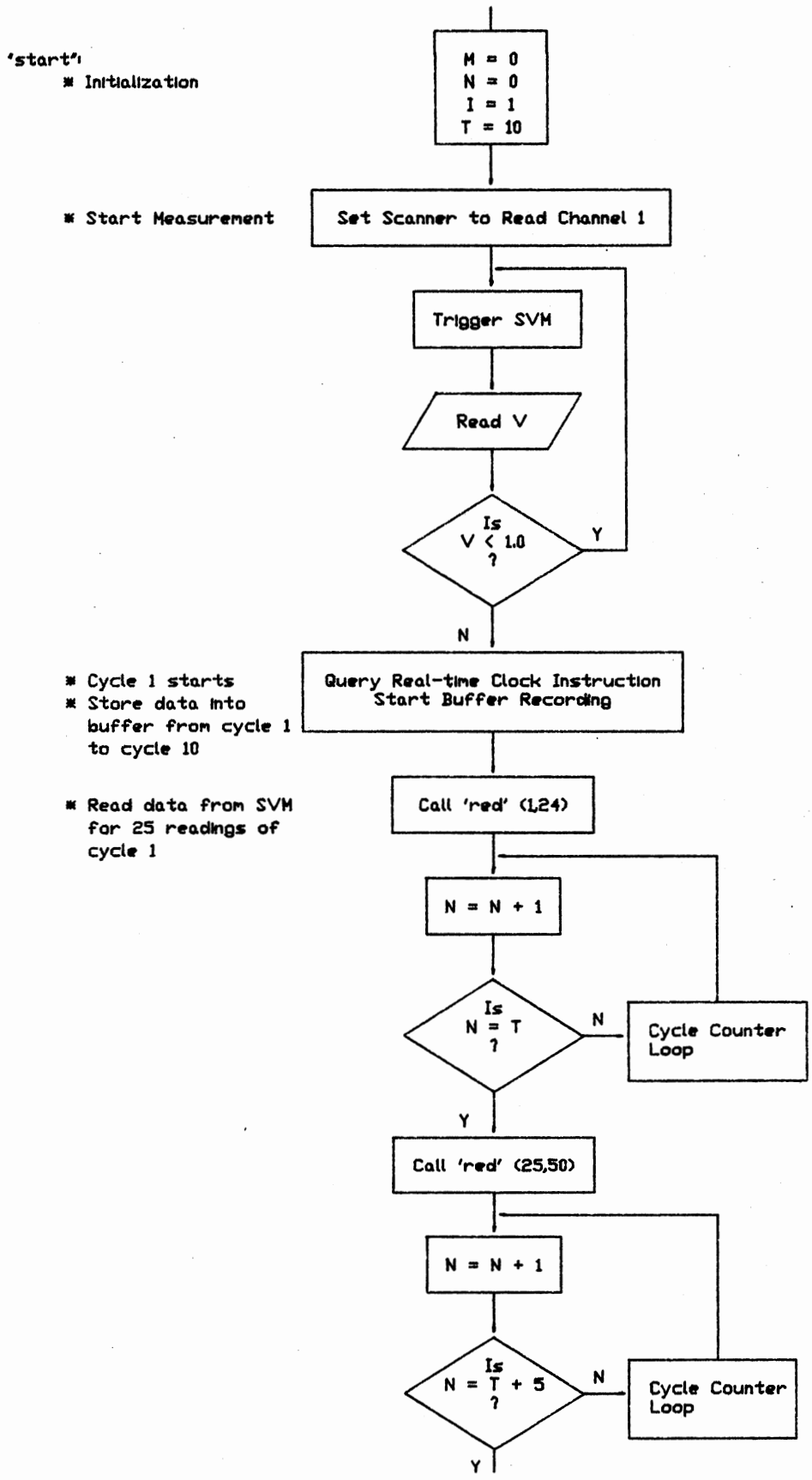
'start':
* Initialization
M = 0
N = 0
I = 1
T = 10
* Start Measurement
Set Scanner to Read Channel 1
Trigger SVM
Read V
Is V < 1.0 ?
Y
N
* Cycle 1 starts
* Store data into buffer from cycle 1 to cycle 10
Query Real-time Clock Instruction
Start Buffer Recording
* Read data from SVM for 25 readings of cycle 1
Call 'red' (1,24)
N = N + 1
Is N = T ?
N
Cycle Counter Loop
Y
Call 'red' (25,50)
N = N + 1
Is N = T + 5 ?
N
Cycle Counter Loop
Y

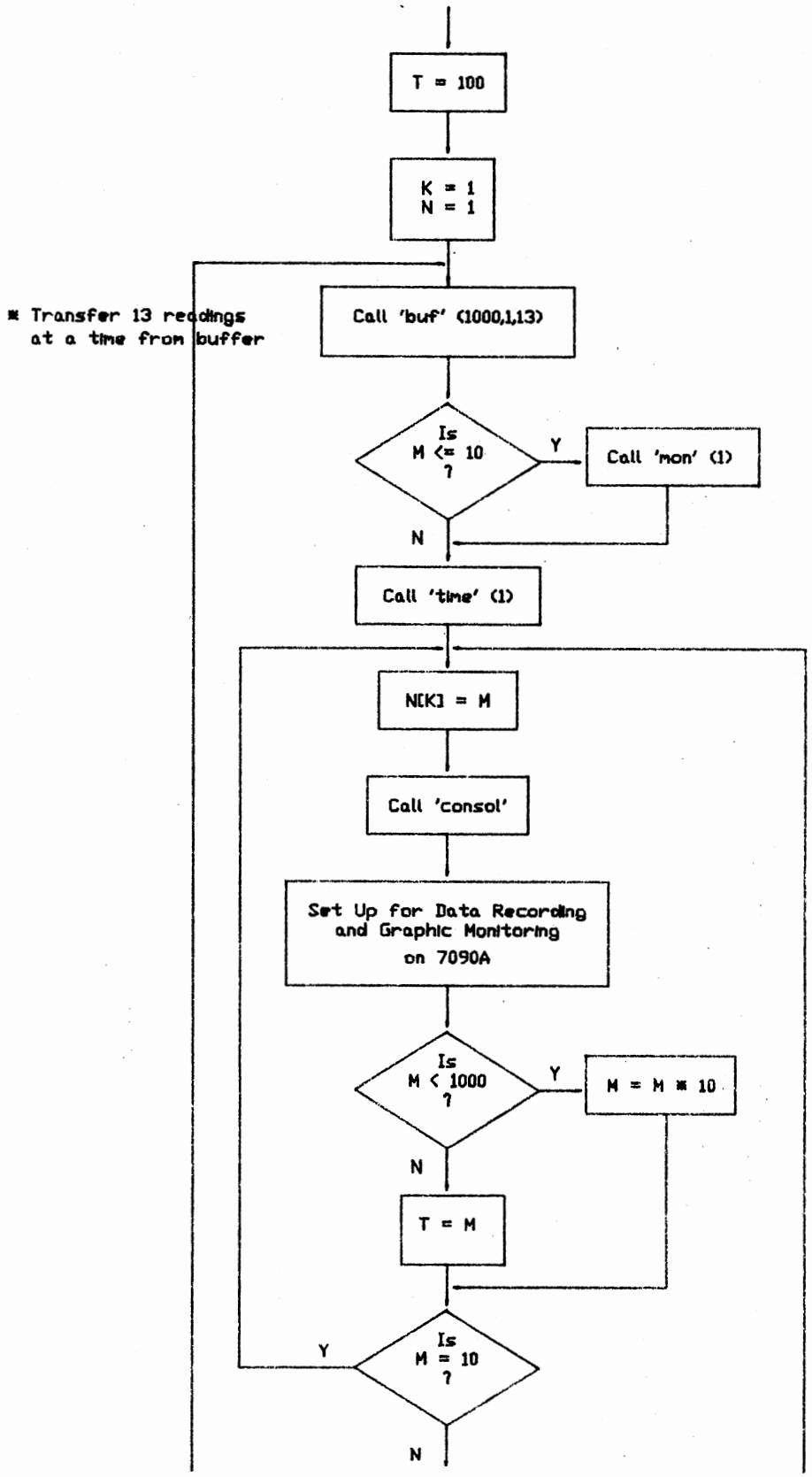
T = 100
K = 1
N = 1
* Transfer 13 readings at a time from buffer
Call 'buf' (1000,1,13)
Is M <= 10 ?
Y
Call 'mon' (1)
N
Call 'time' (1)
N[K] = M
Call 'consol'
Set Up for Data Recording and Graphic Monitoring on 7090A
Is M < 1000 ?
Y
M = M * 10
N
T = M
Is M = 10 ?
Y
N

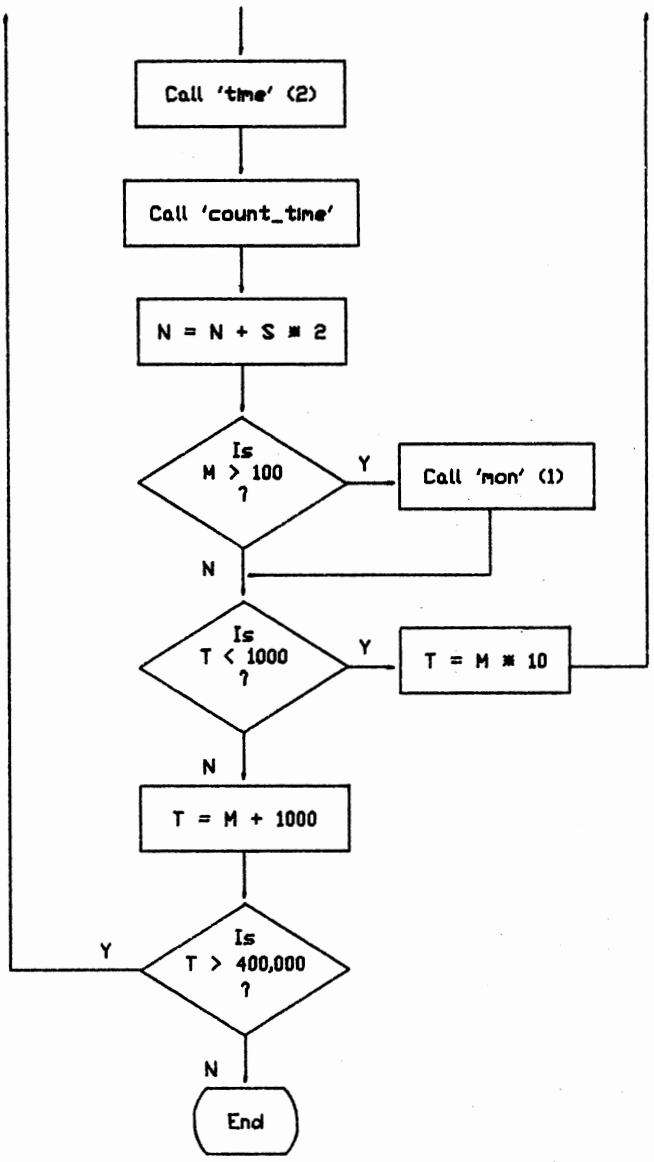
Call 'time' (2)
Call 'count_time'
N = N + S * 2
Is M > 100 ?
Y
Call 'mon' (1)
N
Is T < 1000 ?
Y
T = M * 10
N
T = M + 1000
Is T > 400,000 ?
Y
N
End

Subroutine: mark_tape

Input variables:

G : track number used for the data tape

Output variables:

None

Description: This subroutine formats (marks) the data tape at the specified track number. The tape is marked with an initial file (file 0) of 200 bytes followed by 500 files of 150 bytes each.

Subroutine : 'mark_tape'

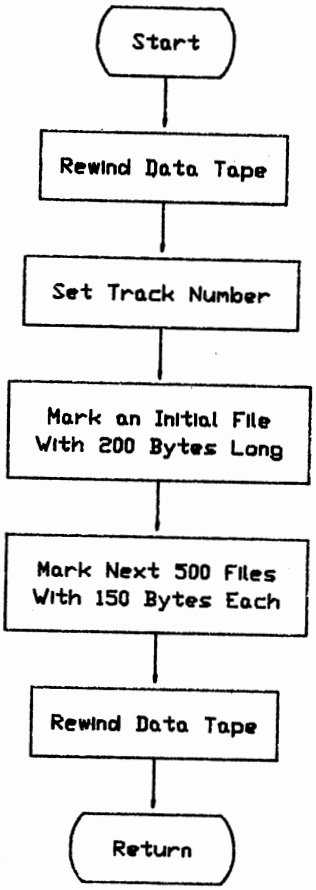

Subroutine: rec_file

Input variables:

K : file number to be used for data storage

M : designated cycle number at which the stored data are measured

P[*] : maximum and minimum voltages of load and strain channels

Q[*] : maximum force at each load cell for upward and downward half of a cycle

H[*] : maximum total restraining force for each half of a cycle

X[*] : horizontal position of the centroid of H[*], measured from the north load cell

Y[*] : vertical position of the centroid of H[*], measured from the middle load cell

Output variables:

None

Description: This routine stores all input data onto tape at a specified file number, K.

Subroutine : 'rec_file'

* Check for number of file if exceeds the capacity of data tape, deduct with 500 from K

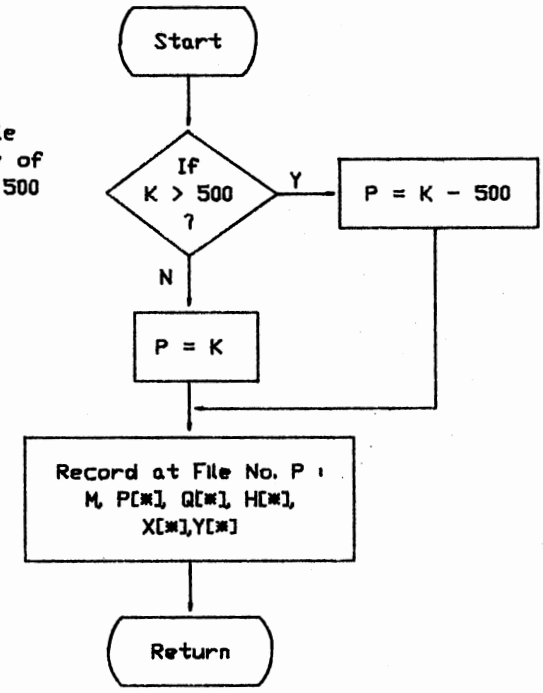

Subroutine: count_time

Input variables:

T[J,I]: a two dimensional array variable that contains the clock time requested by the main program. A value of 1 or 2 for the first subscript indicates the time before the program consolidates data, or the time after the data consolidation is finished, respectively. Values of 1, 2, 3, 4, 5, and 6 for the second subscript indicate year, month, day, hour, minute, and second respectively.

Output variables:

S : total seconds that are used to consolidate data.

Description: This calculates the total amount of time used to consolidate data. If the time period crosses over a month, the subroutine will call another subroutine named 'check_day' to obtain the number of days during that period. The result of this primitive will be stored in a variable called 'S' which is the total number of seconds of consolidation time.

Subroutine : 'count_time'

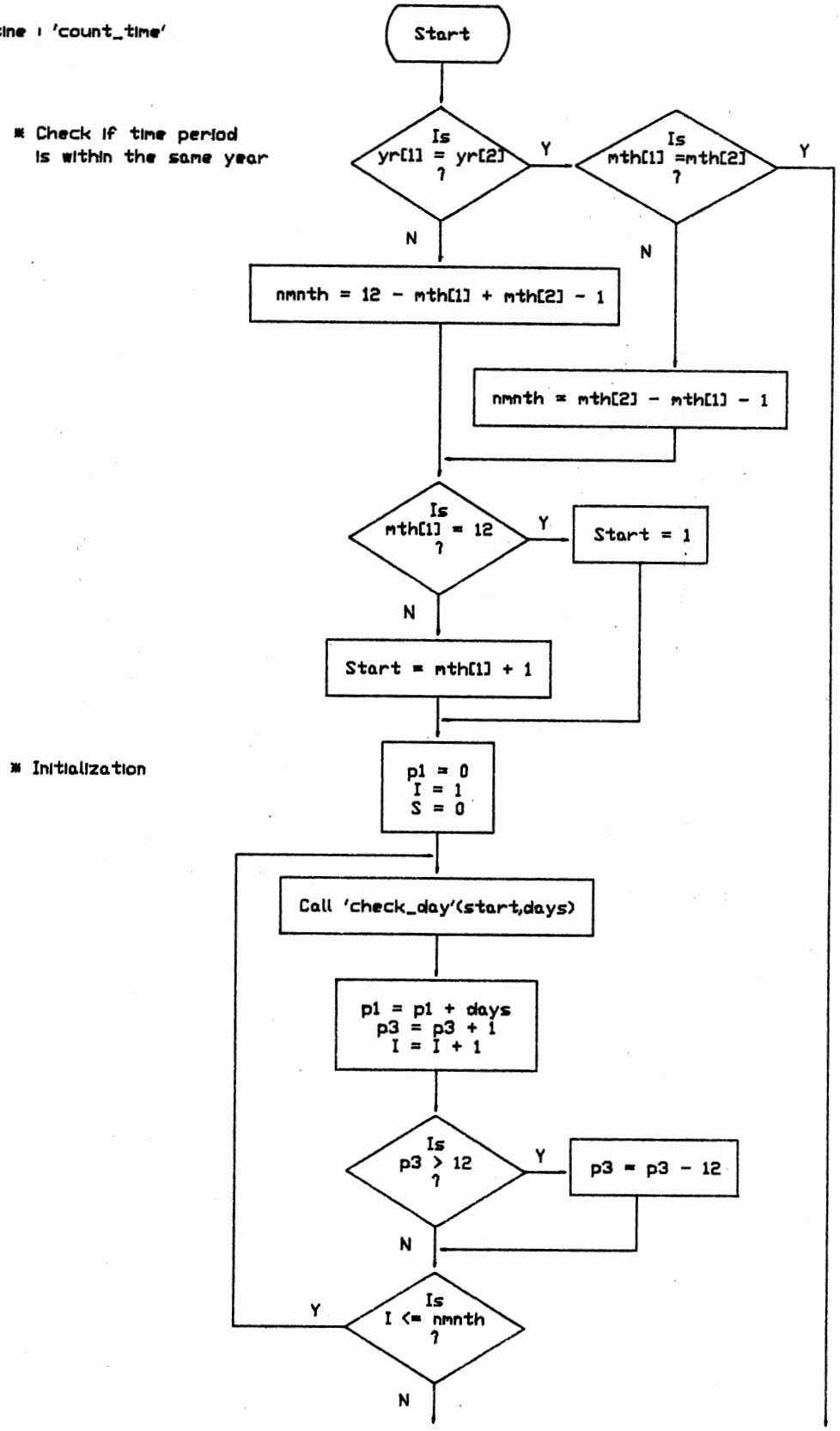

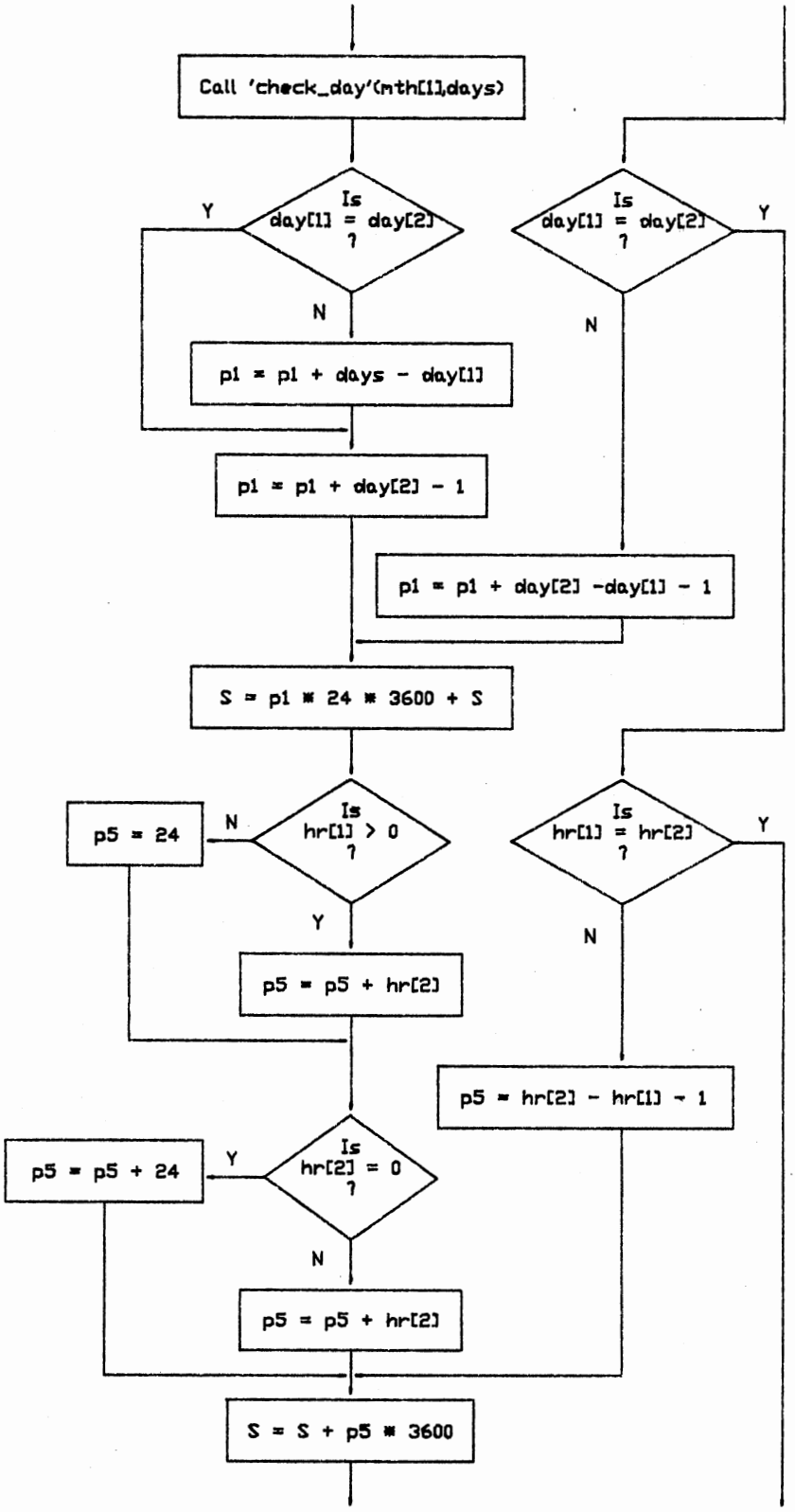
Call 'check_day'(mth[1],days)
Is day[1] = day[2] ?
Y
N
p1 = p1 + days - day[1]
p1 = p1 + day[2] - 1
Is day[1] = day[2] ?
Y
N
p1 = p1 + day[2] -day[1] - 1
S = p1 * 24 * 3600 + S
Is hr[1] > 0 ?
N
Y
p5 = 24
p5 = p5 + hr[2]
Is hr[1] = hr[2] ?
Y
N
p5 = hr[2] - hr[1] - 1
Is hr[2] = 0 ?
Y
N
p5 = p5 + 24
p5 = p5 + hr[2]
S = S + p5 * 3600

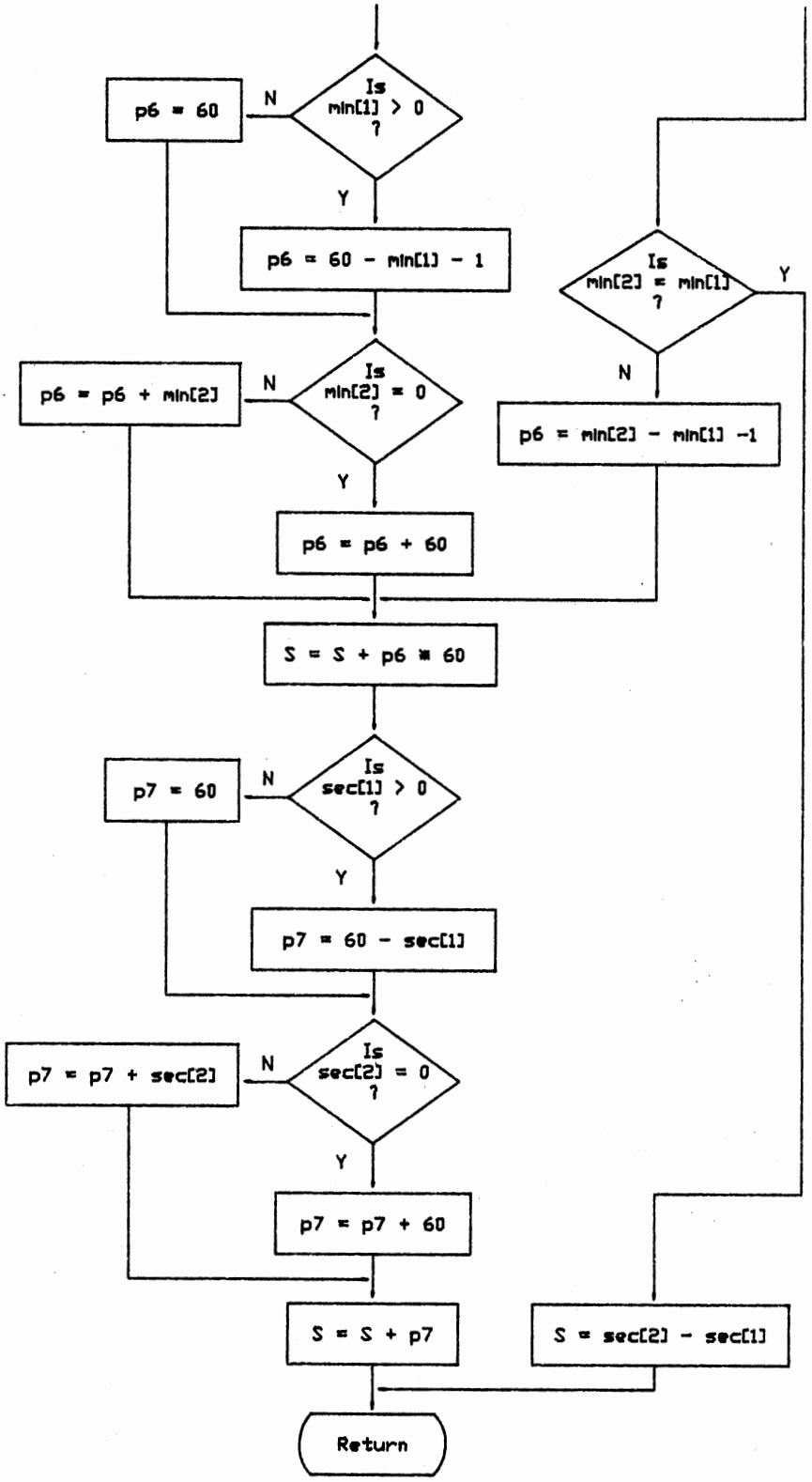
Is min[1] > 0 ?
N
p6 = 60
Y
p6 = 60 - min[1] - 1
Is min[2] = min[1] ?
Y
N
p6 = min[2] - min[1] -1
Is min[2] = 0 ?
N
p6 = p6 + min[2]
Y
p6 = p6 + 60
S = S + p6 * 60
Is sec[1] > 0 ?
N
p7 = 60
Y
p7 = 60 - sec[1]
Is sec[2] = 0 ?
N
p7 = p7 + sec[2]
Y
p7 = p7 + 60
S = S + p7
S = sec[2] - sec[1]
Return

Subroutine: check_day

Input variables:

The only variable is the month number (1-12).

Output variables:

The output is the number of days for that specified month.

Description: This subroutine will compute the number of days contain in a given month. The concept used is that for the month before July, the odd month has 31 days and for the month after July, the odd month has only 30 days. However, if it is February the number of days is 28.

Subroutine : 'check_day'

* February has 28 days

* For month before July, the odd month has 31 days

* For month after July, the odd month has 30 days

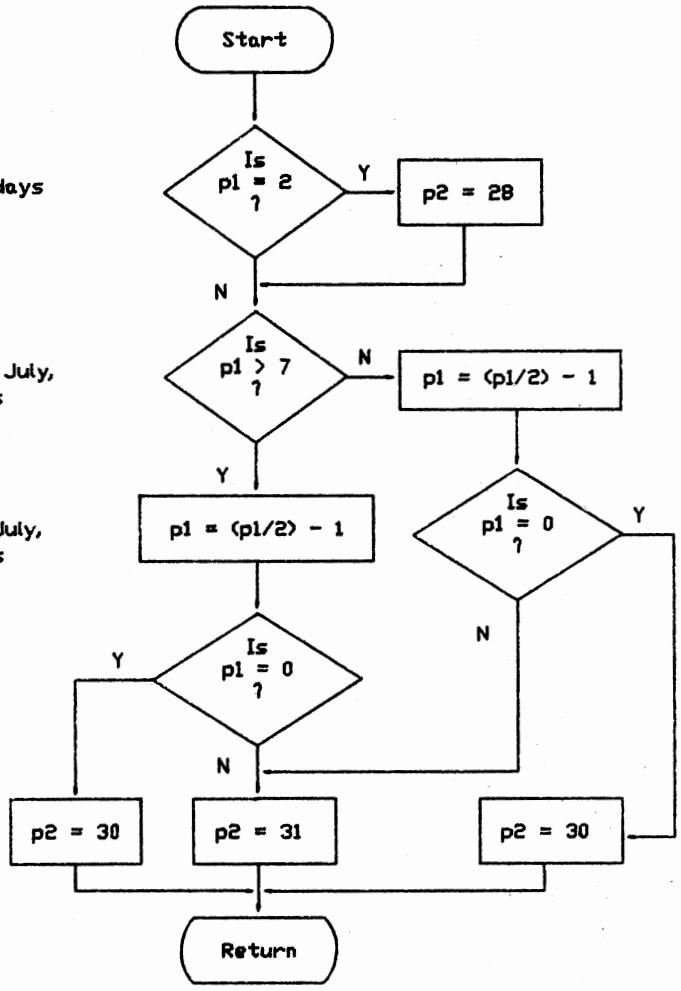

Subroutine: 'time'

Input variables:

p1 : number equals 1 or 2, indicating the start and the end of data consolidation respectively.

Output variables:

T[J,I]: a two dimensional array variable containing clock time. Subscript I equals 1 to 6 for year, month, day, hour, minute, and second respectively. J = p1.

Description: This routine requests clock time from the HP 7090A.

Subroutine : 'time'

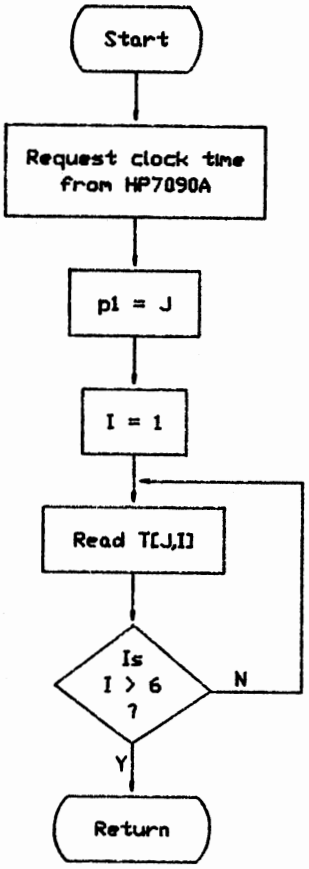

Subroutine: buf

Input variables:

p1 : total number of data sets to be transferred from the buffers, p1 = 1,000

p2 : initial number of data set to be transferred in each cycle

p3 : rate of data transferring per cycle, p3 = 13

Output variables:

A[i] : voltage signal at ith reading from upper-north load cell

B[i] : voltage signal at ith reading from lower-middle load cell

C[i] : voltage signal at ith reading from upper-south load cell

Description: This routine transfers readings from the buffers of the HP 7090A to the computer memory at a rate of 13 data sets per cycle while performing routine cycle counting. The buffers must be cleared before a new measurement sequence can be initiated. Normally, only the first 100 readings are stored for a given measured cycle. Exception: in cycle 10, the last 100 readings are stored.

Subroutine : 'buf'

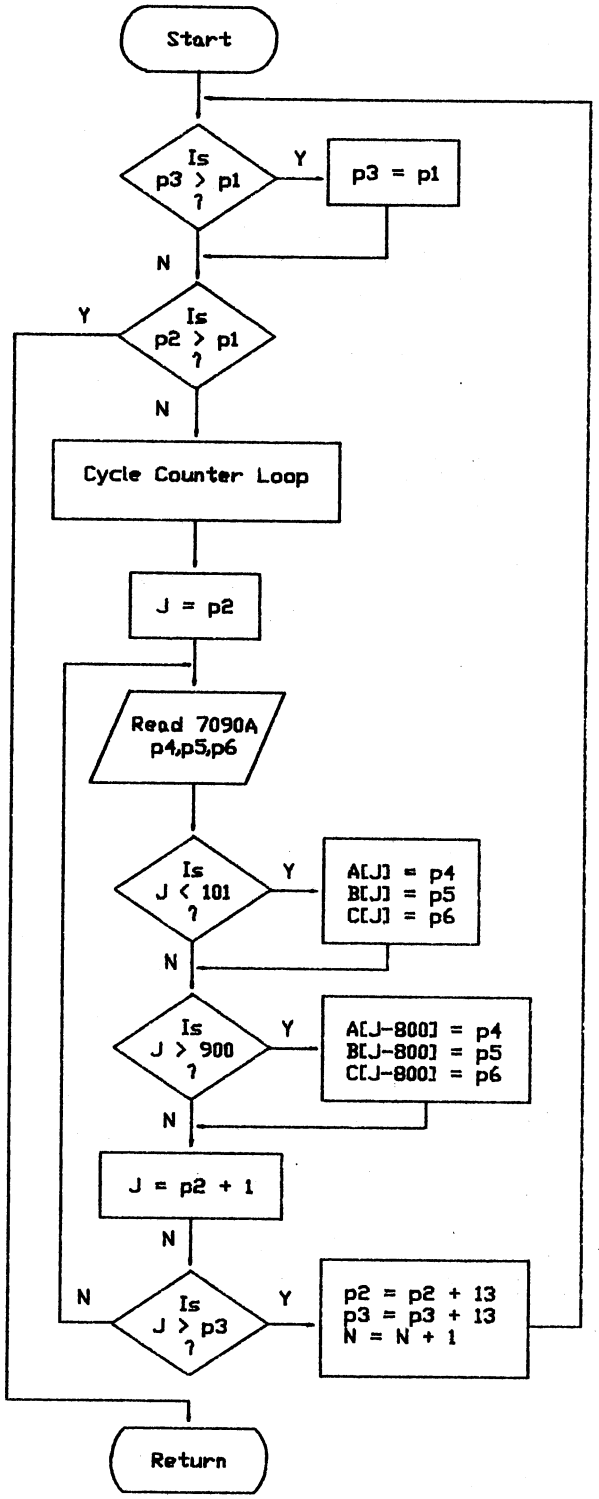

Subroutine: red

Input variables:

p1, p2: the first and the last number of the data set to be read, p2 = p1 + 24

Output variables:

D[i,j]: voltage signal at ith reading from load channel if j = 1 or voltage signal at ith reading from strain channel, if j = 2

Description: This routine alternately reads 25 voltage signals from each of the Pegasus load and strain channels at a specified cycle. For cycle 1 and 10, p1 and p2 are "hard coded" in call statements in the main program. From cycle 100 on, p1 and p2 are calculated and 'red' is called in subroutine 'mon'.

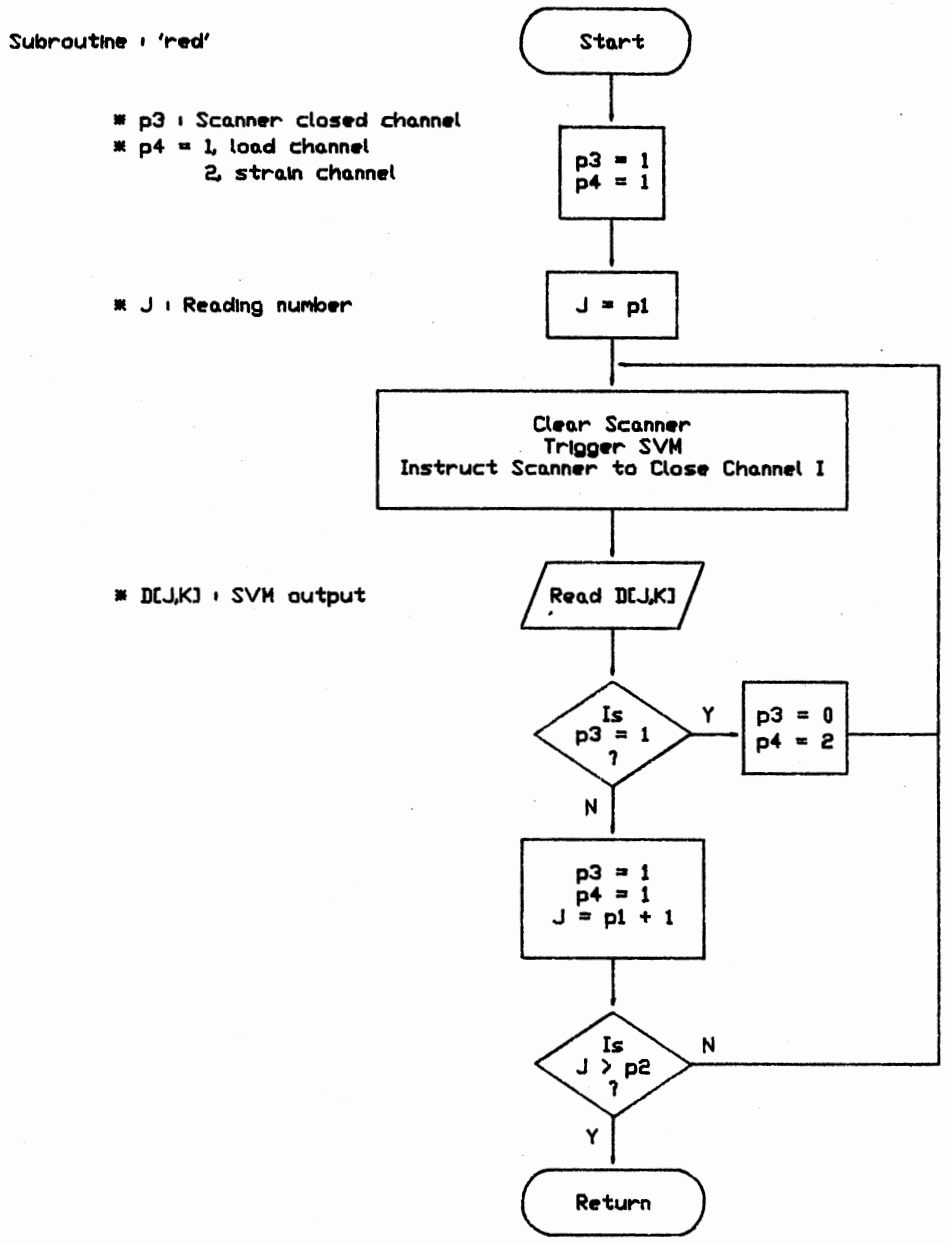
Subroutine : 'red'
* p3 : Scanner closed channel
* p4 = 1, load channel
2, strain channel
* J : Reading number
* D[J,K] : SVM output
Start
p3 = 1
p4 = 1
J = p1
Clear Scanner
Trigger SVM
Instruct Scanner to Close Channel I
Read D[J,K]
Is
p3 = 1
?
Y
p3 = 0
p4 = 2
N
p3 = 1
p4 = 1
J = p1 + 1
Is
J > p2
?
N
Y
Return

Subroutine: mon

Input variables:

T : specified cycle to take measurement readings

Output variables:

None

Description: This monitors the number of cycles. When the cycle count equals T, 'mon' will initiate a measurement sequence by triggering the HP 7090A and by calling subroutine 'red'. The HP 7090A will record 1,000 readings from each of the three load cells for a period of 5 seconds. Subroutine 'red' will read voltage signals from the Pegasus load and strain channels. Subroutine 'mon' counts cycles in order to provide enough time for the buffer of the HP 7090A to be filled.

Subroutine : 'mon'

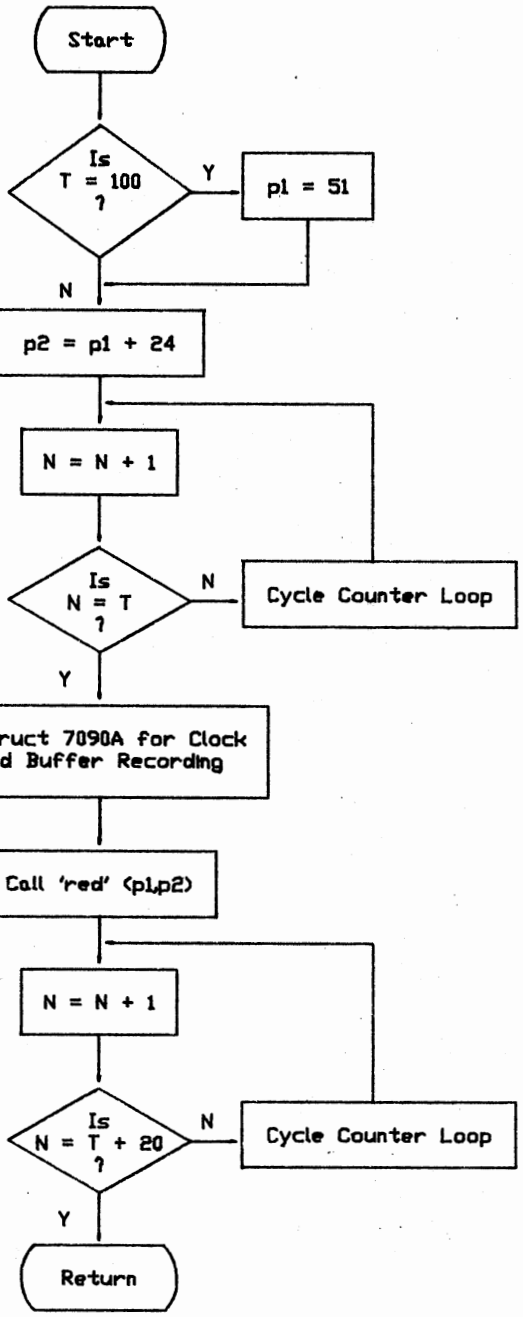

* Measurement Starts

Subroutine: consol

Input variables:

A[i] : voltage signal at ith reading from upper-north load cell

B[i] : voltage signal at ith reading from lower-middle load cell

C[i] : voltage signal at ith reading from upper-south load cell

D[i,j]: voltage signals from load channel and strain channel

M : index of cycle that starts consolidation

Z[1] : horizontal distance between upper load cells, 26.25 in.

Z[2] : horizontal distance between upper and lower load cells, 13.125 in.

Z[3] : vertical distance between upper and lower load cells, 19.0 in.

I[3] : initial reading of A[i]

I[4] : initial reading of B[i]

I[5] : initial reading of C[i]

Output variables:

P[1] : maximum voltage of load channel

P[2] : minimum voltage of load channel

P[3] : maximum voltage of strain channel

P[4] : minimum voltage of strain channel

H[1] : maximum total restraining force for upward loading half of a cycle

H[2] : maximum total restraining force for downward loading half of a cycle

X[1] : horizontal position of H[1] measured from the north load cell

X[2] : horizontal position of H[2] measured from the north load cell

Y[1] : vertical position of H[1] measured from the lower load cell

Y[2] : vertical position of H[2] measured from the lower load cell

Q[1] : maximum of A[i]-I[3] for first half cycle

Q[2] : maximum of B[i]-I[4] for first half cycle

Q[3] : maximum of C[i]-I[5] for first half cycle

Q[4] : maximum of A[i]-I[3] for second half cycle

Q[5] : maximum of B[i]-I[4] for second half cycle

Q[6] : maximum of C{i]-I[5] for second half cycle

Description: This routine finds maximum and minimum values of various input data. In addition, it performs the calculations for the centroid of H[1] and H[2] with respect to reference axes through the upper-north and lower-middle load cells.

Subroutine : 'consol'

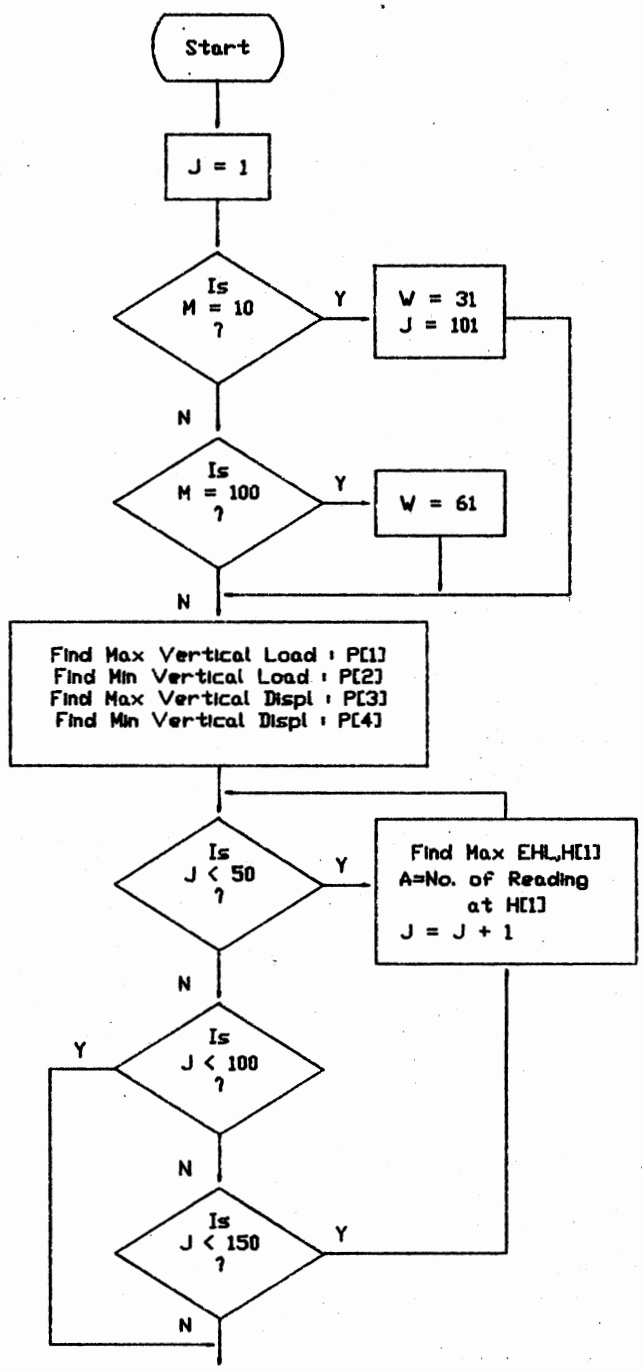

* For first 1/2 cycle

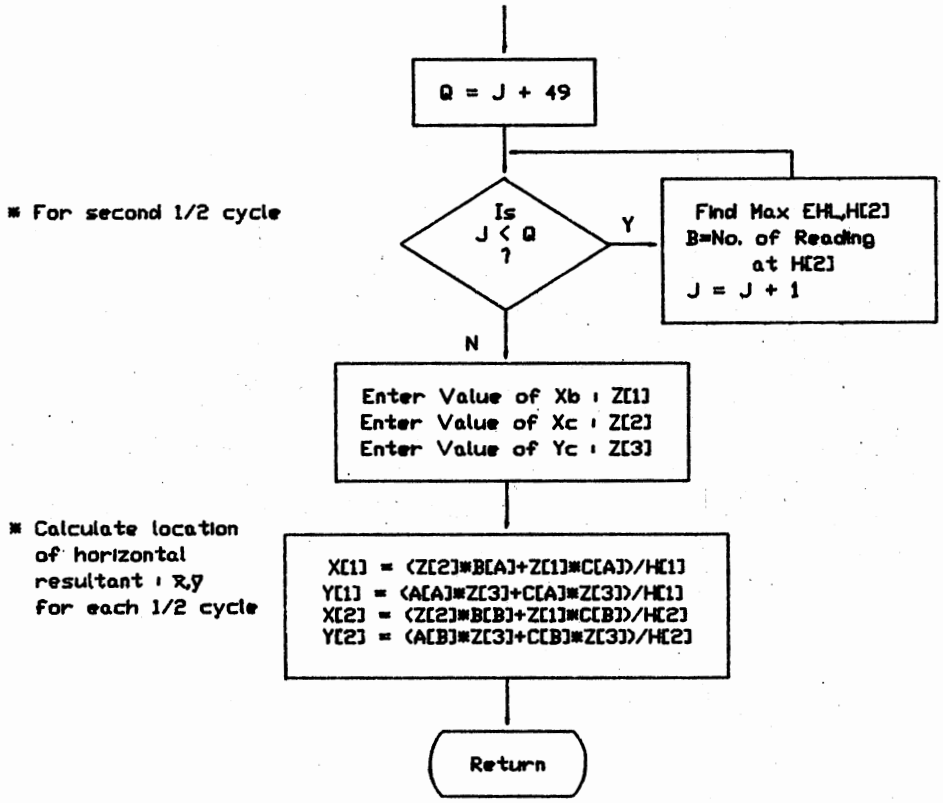
* For second 1/2 cycle
Q = J + 49
Is J < Q ?
Y
Find Max EHL,H[2]
B=No. of Reading at H[2]
J = J + 1
N
Enter Value of Xb : Z[1]
Enter Value of Xc : Z[2]
Enter Value of Yc : Z[3]
* Calculate location of horizontal resultant : x,y for each 1/2 cycle
X[1] = (Z[2]*B[A]+Z[1]*C[A])/H[1]
Y[1] = (A[A]*Z[3]+C[A]*Z[3])/H[1]
X[2] = (Z[2]*B[B]+Z[1]*C[B])/H[2]
Y[2] = (A[B]*Z[3]+C[B]*Z[3])/H[2]
Return

Subroutine: set_plot

Input variables:

None

Output variables:

None

Description: 'set_plot' is called to initialize the plotter on the HP 7090A. The text size is set to be 0.15 in. wide and 0.2 in. thick. The plotting area is scaled to be in the range of -700 to 6,200 plotter units for x-axis and a range of -1300 to 1300 plotter units for y-axis. Both axes are ticked and labeled before the subroutine returns to the calling routine.

Subroutine : 'set_plot'

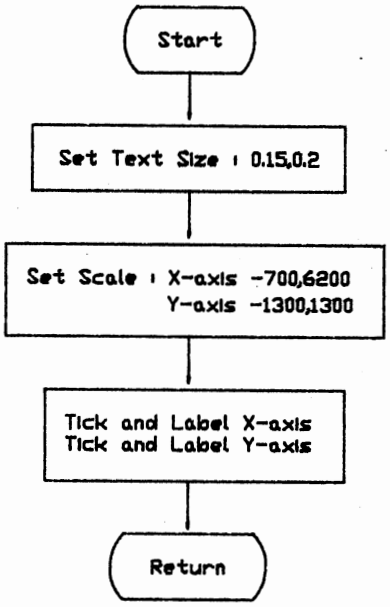

Subroutine: plot

Input variables:

N[K] : designated cycle

H[1] : maximum total restraining force for upward loading half of the cycle

H[2] : maximum total restraining force for downward loading half of the cycle

P[3] : maximum voltage output of strain channel

P[4] : minimum voltage output of strain channel

Q[1] : A[A]-I[3]

Q[2] : B[A]-I[4]

Q[3] : C[A]-I[5]

Q[4] : A[B]-I[3]

Q[5] : B[B]-I[4]

Q[6] : C[B]-I[5]

Output variables:

None

Description: This routine plots log (N[K]) vs. other input variables on HP 7090A. Five different colored pens are used. Pen number and the corresponding data are as follows:

Pen number	Associated data
1	P[3] and P[4]
2	H[1] and H[2]
3	Q[1] and Q[4]
4	Q[2] and Q[5]
5	Q[3] and Q[6]

Subroutine : 'plot'

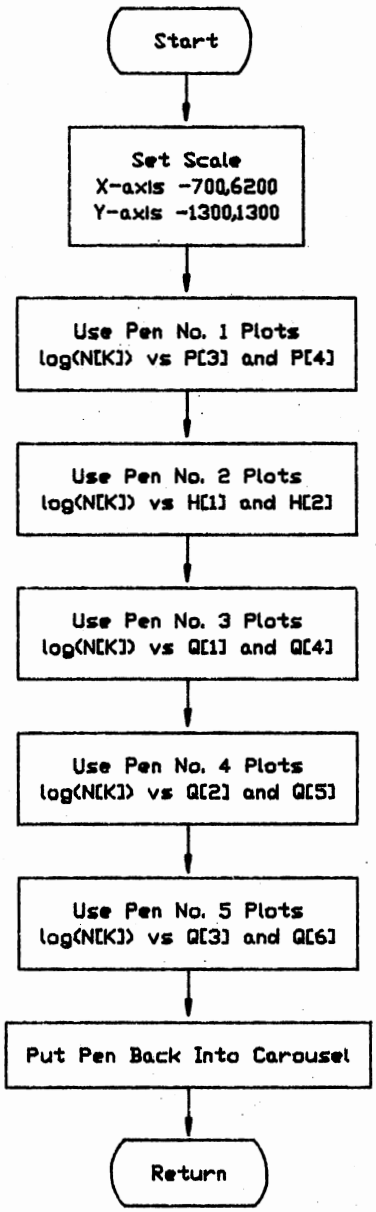

APPENDIX C

LISTING OF COMPUTER PROGRAMS

```
0: gto "INIT"
1: "mark_tape":
2: rew
3: trk 6
4: mrk 1,200
5: mrk 500,150
6: rew
7: ret
8: "rec_file":
9: if K>500;K-500}P;gto +2
10: K}P
11: rcf P,M,P[*],Q[*],H[*],X[*],Y[*]
12: ret
13: "check_day":
14: if p1=2;28}p2;gto +9
15: if p1>7;gto +5
16: p1/2-1}p1
17: if p1=0;30}p2;gto +6
18: 31}p2
19: gto +4
20: p1/2-1}p1
21: if p1=0;31}p2;gto +2
22: 30}p2
23: ret
24: "count_time":
25: 0}p1
26: 1}I
27: 0}S
28: if T[2,1]=T[1,1];gto +3
29: 12-T[1,2]+T[2,2]-1}p2
30: gto +3
31: if T[2,2]=T[1,2];gto +15
32: T[2,2]-T[1,2]-1}p2
33: if T[1,2]=12;1}p3;gto +2
34: T[1,2]+1}p3
35: cll 'check_day'(p3,p4)
36: p1+p4}p1
37: p3+1}p3
38: I+1}I
39: if p3>12;p3-12}p3
40: if I<=p2;gto -5
41: cll 'check_day'(T[1,2],p4)
42: if T[1,3]=p4;gto +2
43: p1+p4-T[1,3]+1}p1
44: p1+T[2,3]-1}p1
45: gto +3
46: if T[1,3]=T[2,3];gto +4
47: p1+T[2,3]-T[1,3]-1}p1
48: p1*24*3600+S}S
49: gto +4
50: if T[1,4]=T[2,4];gto +8
51: T[2,4]-T[1,4]-1}p5
52: gto +4
53: if T[1,4]>0;24-T[1,4]-1}p5;gto +2
54: 24}p5
55: p5+T[2,4]}p5
56: S+p5*3600}S
57: gto +4
58: if T[1,5]=T[2,5];gto +12
59: T[2,5]-T[1,5]-1}p6
60: gto +4
```

```
61: if T[1,5]>0;60-T[1,5]-1}p6;gto +2
62: 60}p6
63: p6+T[2,5]}p6
64: S+p6*60}S
65: if T[1,6]>0;60-T[1,6]}p7;gto +2
66: 60}p7
67: p7+T[2,6]}p7
68: S+p7}S
69: gto +2
70: T[2,6]-T[1,6]}S
71: ret
72: "time":
73: wrt 707,"QW"
74: p1}J
75: for I=1 to 6
76: red 707,T[J,I]
77: next I
78: ret
79: "buf":
80: wrt 707,"D00,1000,0,0;"
81: wrt 707,"QI;"
82: N+1}N
83: dsp "take out data at",p2
84: if p3>p1;p1}p3
85: if p2>p1;gto +12
86: fxd 2
87: trg 724;red 724,V
88: if V>1;trg 724;red 724,V;gto +0
89: if V<1;trg 724;red 724,V;gto +0
90: for J=p2 to p3
91: red 707,p4,p5,p6
92: if J<101;p4}A[J];p5}B[J];p6}C[J]
93: if J>900;p4}A[J-800];p5}B[J-800];p6}C[J-800]
94: next J
95: p2+13}p2;p3+13}p3
96: N+1}N;gto -13
97: ret
98: "red":
99: 1}p3}p4
100: for J=p1 to p2
101: wtb 709,","
102: trg 724
103: wrt 709.3,p3
104: red 724.4,D[J,p4]
105: if p3=1;0}p3;2}p4;gto -4
106: 1}p3}p4
107: next J
108: ret
109: "mon":
110: if T=100;51}p1
111: p1+24}p2
112: dsp "N = ",N
113: N+1}N
114: if N=T;gto +4
115: trg 724;red 724.4,V
116: if V>1;trg 724;red 724,V;gto +0
117: if V<1;trg 724;red 724,V;gto +0
118: wrt 707,"MS1;"
119: cll 'red'(p1,p2)
120: N+1}N
```

```
121: if N=T+20;gto +6
122: if V<1;trg 724;red 724,V;gto +0
123: trg 724;red 724.4,V
124: if V>1;trg 724;red 724,V;gto +0
125: if V<1;trg 724;red 724,V;gto +0
126: gto -6
127: ret
128: "consol":
129: wrt 706,"consol at",N[K]
130: I[3]+I[4]+I[5]}p7
131: 1}J
132: if M=10;31}W;101}J;gto +3
133: if M=100;61}W;gto +2
134: 1}W
135: D[W,1]}p1}p2
136: D[W,2]}p3}p4
137: for I=W to W+24
138: if D[I,1]>p1;D[I,1]}p1
139: if D[I,1]<p2;D[I,1]}p2
140: if D[I,2]>p3;D[I,2]}p3
141: if D[I,2]<p4;D[I,2]}p4
142: next I
143: p1}P[1]
144: p2}P[2]
145: p3}P[3]
146: p4}P[4]
147: if J=1;A[J]+B[J]+C[J]}p5;A[51]+B[51]+C[51]}p6;gto +3
148: A[101]+B[101]+C[101]}p5
149: A[151]+B[151]+C[151]}p6
150: A[J]+B[J]+C[J]}p1
151: if p1<p5;gto +3
152: p1}p5
153: J}A
154: J+1}J
155: if J<=50;gto -5
156: if J<=100;gto +2
157: if J<=150;gto -7
158: J+49}Q
159: A[J]+B[J]+C[J]}p2
160: if p2<p6;gto +3
161: p2}p6
162: J}B
163: J+1}J
164: if J<=Q;gto -5
165: p5-p7}H[1];p6-p7}H[2]
166: A[A]-I[3]}Q[1];B[A]-I[4]}Q[2];C[A]-I[5]}Q[3]
167: (Z[2]*Q[2]+Z[1]*Q[3])/H[1]}X[1]
168: (Q[1]*Z[3]+Q[3]*Z[3])/H[1]}Y[1]
169: A[B]-I[3]}Q[4];B[B]-I[4]}Q[5];C[B]-I[5]}Q[6]
170: (Z[2]*Q[5]+Z[1]*Q[6])/H[2]}X[2]
171: (Q[4]*Z[3]+Q[6]*Z[3])/H[2]}Y[2]
172: ret
173: "set_plot":
174: fxd 0
175: wrt 707,"in;si0.15,0.2"
176: wrt 707,"sc-700,6200,-1300,1300;"
177: wrt 707,"sp1;papu-700,0;"
178: for I=-1100 to 1100 by 100
179: wrt 707,"papd-700,",I,";yt;"
180: next I
```

```
181: wrt 707,"sp2;papu-550,100;"
182: for I=100 to 1100 by 100
183: wrt 707,"papd-550,",I,";yt;"
184: next I
185: wrt 707,"sp3;papu-400,100;"
186: for I=100 to 1100 by 100
187: wrt 707,"papd-400,",I,";yt;"
188: next I
189: wrt 707,"sp4;papu-250,100;"
190: for I=100 to 1100 by 100
191: wrt 707,"papd-250,",I,";yt;"
192: next I
193: wrt 707,"sp5;papu-100,100;"
194: for I=100 to 1100 by 100
195: wrt 707,"papd-100,",I,";yt;"
196: next I
197: wrt 707,"sp2;papu-550,-1100;"
198: for I=-1100 to -100 by 100
199: wrt 707,"papd-550,",I,";yt;"
200: next I
201: wrt 707,"sp3;papu-400,-1100;"
202: for I=-1100 to -100 by 100
203: wrt 707,"papd-400,",I,";yt;"
204: next I
205: wrt 707,"sp4;papu-250,-1100;"
206: for I=-1100 to -100 by 100
207: wrt 707,"papd-250,",I,";yt;"
208: next I
209: wrt 707,"sp5;papu-100,-1100;"
210: for I=-1100 to -100 by 100
211: wrt 707,"papd-100,",I,";yt;"
212: next I
213: wrt 707,"sp1;papu-700,0;papd0,0;"
214: for I=0 to 6000 by 1000
215: wrt 707,"papd",I,",0;xt;"
216: next I
217: wrt 707,"papu-550,600;pd;"
218: for I=0 to 6000 by 1000
219: wrt 707,"papd",I,",600;xt;"
220: next I
221: wrt 707,"papu-550,-600;pd;"
222: for I=0 to 6000 by 1000
223: wrt 707,"papd",I,",-600;xt;"
224: next I
225: wrt 707,"papu0,0"
226: fmt 5,b
227: wrt 707.5,"dt",3
228: wrt 707.5,"sp1;papu-700,1150;lo5;lb11",3
229: wrt 707.5,"papu-700,-1150;lo5;lb-11",3
230: wrt 707.5,"sp1;papu-400,1150;lo5;lb5.0",3
231: wrt 707.5,"papu-550,600;lo18;lb0",3
232: wrt 707.5,"papu-400,50;lo5;lb-5.0",3
233: wrt 707.5,"papu-400,-50;lo5;lb5.0",3
234: wrt 707.5,"papu-550,-600;lo18;lb0",3
235: wrt 707.5,"papu-400,-1150;lo5;lb-5.0",3
236: wrt 707,"di0,1"
237: wrt 707.5,"sp1;pa-700,1250;lo5;lbP3",3
238: wrt 707.5,"sp2;pa-550,1250;lo5;lbH1",3
239: wrt 707.5,"sp3;pa-400,1250;lo5;lbA1",3
240: wrt 707.5,"sp4;pa-250,1250;lo5;lb81",3
```

```
241: wrt 707.5,"sp5;pa-100,1250;lo5;lbC1",3
242: wrt 707.5,"sp1;pa-700,-1250;lo5;lbP4",3
243: wrt 707.5,"sp2;pa-550,-1250;lo5;lbH2",3
244: wrt 707.5,"sp3;pa-400,-1250;lo5;lbA2",3
245: wrt 707.5,"sp4;pa-250,-1250;lo5;lbB2",3
246: wrt 707.5,"sp5;pa-100,-1250;lo5;lbC2",3
247: wrt 707,"di1,0;sp1"
248: wrt 707.5,"pu;pa0,0;lo16;lb1",3
249: wrt 707.5,"pa1000,0;lo16;lb10",3
250: wrt 707.5,"pa2000,0;lo16;lb100",3
251: wrt 707.5,"pa3000,0;lo16;lb1000",3
252: wrt 707.5,"pa4000,0;lo16;lb10000",3
253: wrt 707.5,"pa5000,0;lo16;lb100000",3
254: wrt 707.5,"pa6000,0;lo16;lb1000000",3
255: wrt 707,"papu5800,0"
256: wrt 707.5,"cp0,-1.5;lo6;lb N cycles",3
257: wrt 707,"papu0,0;sp0;"
258: ret
259: "plot":
260: wrt 707,"sc-700,6200,-1300,1300;"
261: wrt 707,"sp1;pa",log(N[K])*1000,",",P[3]*100,";pd;pu;"
262: wrt 707,"sp1;pa",log(N[K])*1000,",",P[4]*100,";pd;pu;"
263: wrt 707,"sp2;pa",log(N[K])*1000,",",H[1]*100+600,"pd;pu;"
264: wrt 707,"sp2;pa",log(N[K])*1000,",",H[2]*100-600,";pd;pu;"
265: wrt 707,"sp3;pa",log(N[K])*1000,",",Q[1]*100+600,";pd;pu;"
266: wrt 707,"sp3;pa",log(N[K])*1000,",",Q[4]*100-600,";pd;pu;"
267: wrt 707,"sp4;pa",log(N[K])*1000,",",Q[2]*100-600,";pd;pu;"
268: wrt 707,"sp4;pa",log(N[K])*1000,",",Q[5]*100-600,";pd;pu;"
269: wrt 707,"sp5;pa",log(N[K])*1000,",",Q[3]*100+600,";pd;pu;"
270: wrt 707,"pa",log(N[K])*1000,",",Q[6]*100-600,"pd;pu;"
271: wrt 707,"sp0;papu0,1200"
272: ret
273: "INIT":
274: 5}C
275: fmt 1,"# of CHAN =",f2.0
276: wrt 706.1,C
277: dsp "NUMBER of CHANNELS =",C;wait 1000
278: dim S[10],U$[10],R[10]
279: wrt 706,"POSSIBLE RANGES:"
280: wrt 706,"3437A DVM:"
281: wrt 706,"0.1V, 1V, 10V"
282: wrt 706,"7090A MEAS SYS:"
283: wrt 706,"0.005V to 10.0V"
284: wrt 706,"NOTE:CH#1 & 2 MUST BE ON 3437A"
285: "cd":
286: fxd 0
287: for I=1 to C
288: .1}S[I]
289: "?"}U$[I]
290: 10}R[I]
291: next I
292: for I=1 to C
293: dsp "SENS for CH#",I;"(V/kip or V/in)?"
294: ent "",S[I]
295: dsp "UNITS for CH#",I,"?"
296: ent "",U$[I]
297: dsp "VOLTAGE RANGE for CH#",I,"?"
298: ent "",R[I]
299: next I
300: dsp "Echo print?(Y=1;N=0)"
```

```
301: ent "",A;if A=0;gto "set"
302: "echo":
303: for I=1 to C
304: fmt 1,"CH#",f3.0,2x,"SENSITIVITY=",f6.2,c10,5x,"VOLTAGE RANGE="
305: wrt 706.1,I,S[I],U$[I],R[I]
306: next I
307: ent "SET-UP DATA  OK? (1=Y,0=N)" ,
308: if A=0;gto "cd"
309: "set":
310: ent "Record Data ?(Y=1,N=0)",F
311: if F=1;ent "Insert tape ; enter track#",G
312: if F=1;ent "Mark tape?(Y=1,N=0)",X
313: if X=1;cll 'mark_tape'
314: trk G
315: dsp "Plot data ? (Y=1,N=0)"
316: ent "",O
317: if O=1;ent "Set up plot ?(Y=1,N=0)",X
318: if X=1;cll 'set_plot'
319: dim T[2,6],I[5]
320: 0}M
321: dim P[4],Q[6],H[2],X[2],Y[2],Z[3]
322: dim N[1000],D[90,2],A[201],B[201],C[201]
323: 26.25}Z[1]
324: 13.125}Z[2]
325: 19}Z[3]
326: 5}P
327: max(R[1],R[2])}r1
328: wrt 724,"R2"
329: if r1<=.1;wrt 724,"R1"
330: if r1>=10;wrt 724,"R3"
331: wrt 724,"T3"
332: fmt 2,c2,",",f6.4,",",f6.4,",",f6.4
333: wrt 707,"IR",R[3],R[4],R[5]
334: wrt 707,"TM0"
335: wrt 707,"TB1,0"
336: fmt 3,fz2.0,"E",z;fmt 4,f
337: "initial_reading":
338: ent "Record initial reading?(Y=1,N=0)",H
339: if H=0;gto "enterI"
340: fxd 2
341: cll 'time'(1)
342: wrt 709.3,0;wait 200;trg 724;red 724.4,I[1]
343: wrt 709.3,1;wait 200;trg 724;red 724.4,I[2]
344: wrt 707,"MS1;";wait 1000
345: wrt 707,"D00,1,0,0;"
346: wrt 707,"Q1;";red 707,I[3],I[4],I[5]
347: if F=1;rcf 0,T[*],I[*];gto "printI"
348: "enterI":
349: for J=1 to 5
350: dsp "enter I",J
351: ent "",I[J]
352: next J
353: "printI":
354: wrt 706,"initial reading"
355: fxd 2
356: wrt 706,"I[1]=",I[1]
357: wrt 706,"I[2]=",I[2]
358: wrt 706,"I[3]=",I[3]
359: wrt 706,"I[4]=",I[4]
360: wrt 706,"I[5]=",I[5]
```

```
361: "start":
362: wrt 707,"TB5,0"
363: fxd 2
364: 0}N
365: 1}I
366: 10}T
367: dso "set up OK_ready to start"
368: wrt 709.3,0
369: trg 724
370: red 724.4,V
371: if V<2.5;gto -2
372: dsp " "
373: wrt 707,"QW;";wrt 707,"MS1;"
374: dsp "N = ",N
375: cll 'red'(1,25)
376: wrt 709.3,0
377: N+1}N
378: dsp "N = ",N
379: if N=T;gto +5
380: trg 724;red 724,V
381: if V>1;trg 724;red 724,V;gto +0
382: if V<1;trg 724;red 724,V;gto +0
383: gto -6
384: cll 'red'(26,50)
385: N+1}N
386: dsp "N = ",N
387: if N=T+5;gto +5
388: trg 724;red 724.4,V
389: if V>1;trg 724;red 724.4,V;gto +0
390: if V<1;trg 724;red 724.4,V;gto +0
391: gto -6
392: 100}T
393: 1}K}M
394: cll 'buf'(1000,1,13)
395: if M<=10;cll 'mon'(1)
396: cll 'time'(1)
397: M}N[K]
398: cll 'consol'
399: if O=1;cll 'plot'
400: if F=1;cll 'rec_file'
401: K+1}K
402: if F=0;gto +6
403: if K<=500;gto +5
404: if G=0;1}G;gto +3
405: dsp "Track 1 is full";wait 1000
406: ent "Insert new tape : enter track#",G
407: cll 'mark_tape'
408: if M<1000;M*10}M;gto +2
409: T}M;gto +2
410: if M=10;gto -13
411: cll 'time'(2)
412: cll 'count_time'
413: N+S*2}N
414: if M>100;cll 'mon'(1)
415: if T<1000;M*10}T;gto -21
416: M+1000}T
417: if T<400000;gto -23
418: end
```

VITA

Charnchai Siriwat

Candidate for the Degree of

Doctor of Philosophy

Thesis: DEVELOPMENT OF A TEST FACILITY FOR EVALUATION OF CONCRETE PAVEMENT JOINTS

Major Field: Civil Engineering

Biographical:

Personal Data: Born in Thailand, January 13, 1947, the son of Aroon and Nanta Siriwat. Married to Panta Pintasut in 1976.

Education: Graduated from Triam Udom Suksa, Bangkok, Thailand, in 1964; received Bachelor of Engineering Degree in Civil Engineering from Chulalogkorn University, Bangkok, Thailand, in 1968; received Master of Science Degree in Civil Engineering from Oklahoma State University in May, 1972; completed requirements for the Doctor of Philosophy Degree at Oklahoma State University in December, 1987.

Professional Experience: Engineer, Telephone Organization of Thailand, 1968 to 1969; Engineer, Bangkok Construction and Management Company, 1969 to 1970; Instructor, Department of Civil Engineering, Institute of Technology and Vocational Education, Thailand, 1973 to 1979; Assistant Professor, Faculty of Engineering, Institute of Technology and Vocational Education, Thailand, 1980 to present.